



UNIVERSITEIT VAN PRETORIA  
UNIVERSITY OF PRETORIA  
YUNIBESITHI YA PRETORIA

# **The effect of scale and shape on the strength of Merensky Reef samples**

**By**

**Stephen Bruce Williams**

**A dissertation submitted in partial requirements for the  
degree Masters of Engineering**

**Faculty of Engineering**

**University of Pretoria**

**April 2000**



## Declaration

I declare that this dissertation is my own work. It is being submitted for the Degree of Engineering in the faculty of Mining Engineering at the University of Pretoria. It has not been submitted before for any degree or examination at any other university.

A handwritten signature in black ink that reads "William" with a large, sweeping underline.

25/02/00

STEPHEN BRUCE WILLIAMS

DATE

## Abstract

In general, as the uniaxial compressive strength of rock samples is tested, the uniaxial strength of the rock decreases with increasing sample size until a strength is reached beyond which no further decrease in strength is observed for further increases in size. The size at which this occurs was termed the critical size by Bieniawski (1968) and the corresponding strength the critical strength. Once these values are obtained no significant changes in strength may be expected as a result of further volume changes. For the purposes of pillar design, this strength should be adjusted to account for other factors that affect pillar strength, the main factors being the width to height ratio ( $w/h$ ) effect, jointing and contact conditions.

Further test work on Merensky Reef was required to clarify the;

1. values of it's critical size and strength
2. effect of the  $w/h$  on it's strength
3. effect of the frictional contacts between the reef and the surrounding rock on the reefs uniaxial strength

These results could then be integrated into a holistic pillar design methodology to improve current pillar designing practices.

These effects were examined through the laboratory testing of samples originating from Amandelbult Platinum mine.

A critical strength of approximately 110 MPa was obtained for samples with diameters, 130 - 250 mm ( $w/h = 1$ ). Increasing the frictional contacts between sample and loading platens was found to increase the sample's strength. A marked difference was found between the *insitu* and laboratory contact friction angles for Merensky Reef. The *insitu* contact friction angle was found to be approximately 2.5 times larger than the laboratory contact friction angle.

The uniaxial strength increased linearly with increasing  $w/h$  ratios up to a  $w/h$  ratio of 6. For  $w/h$  ratios greater than 6 the strength continued to increase with increasing  $w/h$  ratios, but no curve could be acceptably fitted to the data to describe this trend.

The results of this study can be applied to mine pillar design in the Bushveld Igneous complex.

## Opsomming

In die algemeen, wanneer die eenassige druksterkte van rotsmonsters bepaal word, sal die sterkte van die rots afneem terwyl die rots volume vergroot, totdat 'n sterkte bereik word waar geen verdere vermindering in sterkte waargeneem kan word nie. Die toets monster afmetings waar dit plaasvind word volgens Bieniawski (1968) die kritieke grootte genoem en die ooreenstemmende sterkte die kritieke sterkte. Wanneer hierdie waardes bereik word, sal geen beduidende verandering in die sterkte verwag word nie. Vir pilaarontwerp, moet die kritieke sterkte aangepas word om ander faktore ook in ag geneem wat

pilaarsterkte beïnvloed. Die breedte-tot-hoogte verhouding ( $w/h$ ), naatvorming en kontakwryingstoestande, is die belangrikste faktore.

Toetswerk op die Merensky Rif is uitgevoer om die volgende aspekte to ondersoek:-

1. Kritieke grootte en sterkte waardes,
2. die uitwerking van die breedte-tot-hoogte verhouding op die sterkte,
3. die effek van die wryingskontak tussen die rif-rots en die omgewingrots op die eenasige druk sterkte van die rif-rots.

Hierdie resultate kan dan ge-integreer word in 'n holitiese myn pilaarontwerp metodologie, om die pilaarontwerp praktyk te verbeter.

Hierdie resultate is bepaal deur laboratoriumtoetse op rots monster wat van Amandelbult Platinum myn afkomstig is.

'n Kritieke sterkte van ongeveer 110 MPa is bepaal vir rots monsters met 'n deursnee van 130 - 250 mm ( $w/h = 1$ ). Deur die wrywingskontak tussen monsters en las-plate te vergroot is daar gevind dat die eenassige druksterkte toeneem. 'n Merkbare verskil tussen *in-situ* en laboratorium kontakwrywing-hoeke is waargeneem. Die gemete *in-situ* kontakwrywing-hoek was ongeveer 2.5 keer groter as die gemete laboratorium kontakwrywing-hoek.



Die eenassige druksterkte van die toets monsters het liniêr verhoog met 'n vergroting van die w/h verhouding. Waar die w/h verhouding meer as 6 is, het die sterkte verder toegeneem as gevolg van die verhoogde w/h verhouding. Geen wiskundige verwantskap kon afgelei word van die toets resultate om die tendens te beskryf nie.

Die resultate van die navorsing kan toegepas word by die ontwerp van mynpilare in die Bosveldstollings kompleks.

# Contents

<b>DECLARATION.....</b>	<b>3</b>
<b>ABSTRACT.....</b>	<b>4</b>
<b>OPSOMMING.....</b>	<b>5</b>
<b>CONTENTS.....</b>	<b>8</b>
<b>LIST OF FIGURES .....</b>	<b>10</b>
<b>LIST OF TABLES .....</b>	<b>11</b>
<b>1 INTRODUCTION.....</b>	<b>12</b>
<b>2 PROBLEM STATEMENT AND OBJECTIVE.....</b>	<b>15</b>
<b>3 LITERATURE REVIEW.....</b>	<b>16</b>
3.1 THE EFFECT OF SCALE ON STRENGTH AND DEFORMATION .....	16
3.2 THE EFFECT OF W/H AND CONTACT FRICTION ANGLE ON STRENGTH.....	28
3.3 PILLAR STRENGTH EQUATIONS.....	29
3.4 CONCLUSION.....	35
<b>4 RESEARCH METHODOLOGY.....</b>	<b>37</b>
4.1 INTRODUCTION.....	37
4.2 SAMPLE PREPARATION.....	38
4.3 TESTING PROCEDURE .....	40
<b>5 EFFECT OF SCALE .....</b>	<b>43</b>
5.1 INTRODUCTION.....	43
5.2 THE EFFECT OF SCALE ON STRENGTH.....	43
5.3 THE EFFECT OF SCALE ON SAMPLE FAILURE PATTERN.....	45
5.4 CONCLUSION.....	48
<b>6 EFFECTS OF W/H AND THE CONTACT FRICTION ANGLE .....</b>	<b>50</b>
6.1 INTRODUCTION.....	50
6.2 THE EFFECT OF W/H ON STRENGTH.....	50
6.3 THE EFFECT OF W/H ON SAMPLE FAILURE PATTERN .....	54



6.4	THE EFFECT OF THE FRICTIONAL CONTACTS ON STRENGTH.....	55
6.5	CONCLUSIONS .....	57
7	CONCLUSIONS.....	59
8	ACKNOWLEDGEMENTS.....	60
9	REFERENCES.....	61
	APPENDICES: TESTS AND RESULTS.....	67
	APPENDIX A: STANDARD TESTS .....	68
	APPENDIX B : FRICTION ANGLE TESTS.....	72
	APPENDIX C : SCALE EFFECT TESTS.....	73
	APPENDIX D : W/H EFFECT TESTS.....	74



## List of figures

FIGURE 3-1: SURFACE-EFFECTS ON STRENGTH OF MERENSKY REEF .....	21
FIGURE 3-2: SCALE EFFECTS OBSERVED FOR MERENSKY REEF .....	21
FIGURE 3-3: THE SIZE EFFECT OF TWO UNIAXIALLY LOADED, NOTCHED-CORES .....	23
FIGURE 3-4: SCALE EFFECT AS OBSERVED FOR DIFFERENT ROCK TYPES .....	27
FIGURE 3-5: SCALE EFFECTS ON COAL.....	28
FIGURE 3-6: A CONCEPTUAL DIAGRAM OF THE EFFECT OF FRICTIONAL END RESTRAINT ON THE CONFINEMENT OF A SAMPLE, DEPENDING ON ITS W/H.....	29
FIGURE 3-7: AN IDEAL PILLAR SYSTEM DESIGN FLOWCHART .....	35
FIGURE 4-1: CORING OF 54 MM MERENSKY REEF SAMPLES, USING DRILL RIG IN A HAULAGE. ....	38
FIGURE 4-2: O. J. MABENA OF CSIR MININGTEK CUTTING CORE TO THE REQUIRED TEST SIZE. ....	39
FIGURE 4-3: SAMPLE GRINDING, CSIR MININGTEK.....	39
FIGURE 4-4: TEST SETUP SHOWING SAMPLE WITH STRAIN GAUGES AND TRANSDUCERS.....	42
FIGURE 5-1: THE STRENGTH – SIZE RELATION FOR MERENSKY REEF SAMPLES FROM AMANDEBULT PLATINUM MINE.....	44
FIGURE 5-2: THE STRENGTH – SIZE RELATION FOR MERENSKY REEF FROM AMANDEBULT AND IMPALA PLATINUM MINES.....	45
FIGURE 5-3: AN INTACT SAMPLE (DIAMETER = 126 MM, W/H = 1:1) BEFORE TESTING.....	47
FIGURE 5-4: THE SAMPLE IN FIGURE 5-3 AFTER TESTING SHOWING FAILURE ALONG A PLANE.....	47
FIGURE 5-5: SCHEMATIC REPRESENTATION OF FAILURE DEVELOPMENT IN CHARCOAL-GREY- GRANITE .....	48
FIGURE 6-1: THE STRENGTH – W/H RELATIONSHIP FOR MERENSKY REEF FROM AMANDEBULT PLATINUM MINE, FOR CYLINDERS OF DIAMETER = 250 MM. ....	52
FIGURE 6-2: ADDITIONAL W/H TESTS DONE ON 77MM SAMPLES.....	53
FIGURE 6-3: CONCENTRIC-FRACTURING ARISING FROM PLATEN INDENTATION EFFECTS .....	54
FIGURE 6-4: A CONCEPTUAL DIAGRAM OF THE EFFECT OF FRICTIONAL END RESTRAINT ON THE CONFINEMENT OF A SAMPLE, DEPENDING ON ITS W/H.....	55
FIGURE 6-5: GEOMETRY OF FLAC MODEL TO TEST THE EFFECT OF THE CONTACT FRICTION ANGLE ON THE STRENGTH OF LABORATORY MODEL PILLARS. ....	56
FIGURE 6-6: THE EFFECT OF THE CONTACT FRICTION ANGLE ON THE W/H EFFECT, ON THE BASIS OF NUMERICAL MODELLING.....	56
FIGURE A-1: PRINCIPAL STRESS DIAGRAM FOR MERENSKY REEF.....	69



## List of Tables

TABLE 1: COMPILATION OF SCALE EFFECT DATA ON COMPRESSIVE STRENGTH.....	17
TABLE 2: DIMENSIONS AND THE NUMBER OF MERENSKY REEF SAMPLES TESTED. ....	40
TABLE 3: LINEAR FUNCTIONS (EQUATION 3-4) FITS TO $w/h \leq 6$ .....	51
TABLE 4: RESULTS OF A POWER FORMULA (EQUATION 3-3) FITS TO $w/h \leq 6$ .....	51
TABLE 5: UNIAXIAL AND TRIAXIAL STRENGTH TESTS MERENSKY REEF SAMPLES. ....	68
TABLE 6: SCALE EFFECT TESTS ON MERENSKY REEF. ....	73
TABLE 7: RESULTS OF $w/h$ TESTS FOR SERIES 1.....	74
TABLE 8: RESULTS OF $w/h$ TESTS FOR SERIES 2.....	76

# 1 Introduction

South Africa's platinum mines are situated in the Bushveld Igneous Complex (BIC), which extends for 400 kilometres in the Northern Province and contains the world's largest known deposits of platinum group metals (PGMs) - platinum, palladium, rhodium, ruthenium, iridium and osmium. 'The BIC was formed some 2 billion years ago when vast quantities of molten rock from the earth's mantle were brought to surface through long vertical cracks in the earth's crust. Crystallisation of different minerals at different temperatures from the lava, resulted in the formation of a structure rather like a layered cake consisting of distinct mineral strata, including three PGM-bearing reefs, the Merensky, UG2 and Platereef (The Chamber of Mines, 1999).'

'The BIC can be divided into northern, eastern and western sections. In the western BIC, where the major platinum mines are situated, the reef occurs in a narrow, 25- centimetre-wide PGM rich band bounded by two thin chromite layers. This pattern falls away in other areas resulting in the reefs diverging between the chromite bands until it is many metres wide. The Merensky Reef is characterised by its high PGM grades and the high ratio of platinum to the other PGMs, especially those of major importance like palladium and rhodium (Chamber of Mines, 1999).'

The mining of platinum ores is similar to gold mining. The ore body is a thin, tabular reef covering an extensive area. This enables a progressive method of mining - the reef is drilled and blasted to

advance the face, support being installed for local control of the hanging wall and pillars being cut out of the reef for excavation stability purposes. On the mine Amandebult these pillars vary in size from large barrier pillars (15m by 15m) to small, in-stope crush pillars (4m by 4m).

To improve pillar design methods, this study aims to do further work on the understanding of how samples of pillar material are influenced by size, geometry and the frictional contacts between the sample and its loading platens.

In general, it is accepted that the values of the strength of rock decrease with increasing specimen size (York and Canbulat, 1998). Evidence in the literature shows that, for design problems at mine pillar scale, the strength size relation has flattened out and no further decrease in strength is apparent due to increasing pillar size. The size at which the curve flattens was termed the *critical size* by Bieniawski and van Heerden (1975), and the corresponding strength, the *critical strength*. Once this value has been obtained, no further significant changes in strength may be expected as a result of volume changes. For the purposes of pillar design, this strength should be adjusted to account for other factors that affect pillar strength, the main factors being the pillar's width to height ratio ( $w/h$ ), jointing and contact conditions with the surrounding strata (G. York *et al.*, 1999).

Baker-Duly (1995) did work to define the strength size relationship, the effect on strength of the  $w/h$  and contact friction angle between specimen and loading platen for Merensky Reef and two other BIC

rock types. He tested cylindrical rock samples, with a w/h ratio of 1, up to a maximum diameter of 150 mm, under laboratory uniaxial loading conditions as prescribed by the International Society of Rock Mechanics (ISRM). Similar samples were then also tested under conditions in which there was no frictional contact between the sample and the loading platens. From these tests he concluded that Merensky Reef was scale dependent for both loading conditions. The critical strength for the laboratory conditions was estimated to be 104 MPa.

To test the effect of w/h ratio on strength Baker-Duly tested the samples of the rocks at 54 mm diameter at w/h ratios of 1/3, 1, 2, 3 and 4. 100 mm diameter samples were tested at w/h ratios of 1, 2, and 4. The two diameters were chosen for correlation purposes, as uncertainty existed whether the large grain size of the reef would influence the results at the smaller diameter. The pillar strength was found to increase linearly with the pillar's w/h.

## 2 Problem statement and objective

There is insufficient data to define the critical strength of the Merensky Reef. It is necessary to determine what the effects of various sample geometries have on Merensky Reef sample strengths so that these effects can be estimated for pillars.

Therefore the study aims to determine the;

- value for the critical strength and size of the Merensky Reef.
- strengthening effect of increasing the w/h ratio on Merensky reef samples.
- effect of scale and geometry on the deformation characteristics, and breakage pattern of Merensky Reef samples tested.

## 3 Literature review.

### 3.1 The effect of scale on strength and deformation

Different rock types have different critical strengths or no critical strength at all, as the effect of scale on strength differs between various rock types. A literature study was carried out to obtain information on previous studies done to examine the scale effect on various rock types.

The effect of scale on the uniaxial compressive strength (UCS) observed on various rock types displays differing and contradictory trends these include:

- Strength decreases with increasing sample size e.g. Hoek and Brown, 1980; Herget, 1988; Kostak and Bilenstein, 1971; Kramadibrat and Jones, 1993.
- Strength initially increases and then decreases with increasing sample size e.g. Pratt *et al.*, 1972; Jackson and Lau, 1990; Baker-Duly, 1995.
- Strength increases with increasing sample size e.g. Stephenson and Triantafilides, 1974.
- Strength is essentially unaffected by volume changes e.g. Hodgson and Cook, 1970; Hudson *et al.*, 1971.

A compilation of hard rock test results on the scale effect phenomena are presented in Table 1.



Table 1: Compilation of scale effect data on compressive strength (after Baker-Duly, 1995).

Rock Type	Studied by	Date	Size Effect (Y/N)	Size Range (mm)	Shape	Length/Diameter	Remarks
Marble	Mogil	1962	Yes	40 – 200	Prismatic	2	
Granite	Lundborg	1966	Yes	20 – 60	Cylindrical	1	1 mm cardboard sheet placed between contact surfaces
Norite	Bieniawski	1968	Yes	13 – 178	Cylindrical	1	
Matinenda Sandstone	Kostak & Bleiestein	1970	Yes	54 – 238	Cylindrical	2	
Quartzitic shale, Main Reef Quartzite	Hodgson & Cook	1970	No	5.6 – 152.3	Cylindrical	3	Uniform loading, Machine stiffness equal to specimen
Quartz – Diorite	Pratt et al	1971	Yes	80 – 108 114 – 305	Tri.Prismatic Cylindrical	>1.5	Peak stress reduced by a factor of 10
Georgia Cherokee Marble	Hudson et al	1971	No	19 – 101	Cylindrical	0.33, 1.0, 3.0	
Devonian Sandstone Concrete	Dhir & Sangha	1973	Yes	25.4 – 101.8	Cylindrical	2.5	Strength increases and then decreases for both materials
Tonalite, Granite, Limestone	Stephenson & Triandafillidis	1974	Yes	2.5 – 15.2	Cylindrical	2	
Siderite, Quartz-Diorite	Herget & Unrug	1976	Yes	22 – 241 – 41	Cylindrical	2	Results obtained from triaxial tests included broken siderite samples.
Marble, Limestone, Granite, Basalt, Norite, Gabbro, Quartz-Diorite	Hoek & Brown	1980	Yes	10 - 200	?	Various	
Kayenta Sandstone	Swolfs	1983	No	19 - 146	Cylindrical	2	Uniform loading
Karoo Sandstones	Madden	1984	No	24 - 100	Cylindrical	w/h 1-8	
Lac du Bonnet Granite	Jackson & Lau	1990	Yes	33 - 294	Cylindrical	2	
Metadiabase & Basalt	Panek & Fannon	1992	Yes	28 - 145	Cylindrical	2	Sample ends lubricated
Basaltic, Porphyry	Kramadibrata & Jones	1993	Yes	30 - 150	Cylindrical	2.5	Sample ends lubricated
Anorthosite, Merensky Reef	Duly & York	1995	Yes	12 - 150	Cylindrical	1	Anorthosite showed no scale effect.

Notes:

- All results were obtained under standardised (ISRM) testing procedures, unless stated otherwise.



The reasons for such contradictory and differing trends observed on strength due to the effect of scale complex. They include heterogeneities, Weibull's (1939) Weakest Link Theory, the effects of stored strain energy, surface effects and the increased stress gradients in the specimen due to non-uniform loading conditions (Baker-Duly, 1995). The extent to which these factors act or interact with one another is not fully understood, and thus no one theory at present is able to explain why such trends arise.

Weibull (1939) developed a plausible explanation to explain the scale effect from a statistical theory known as the "Weakest Link Theory". The theory considers the random distribution of micro cracks or flaws within a sample. The sample, which is considered to consist of a series of links, is believed to be as strong as its weakest link or flaw. The greater the sample size, the greater the probability of the inclusion of weaker flaws and hence a diminishing effect on strength is expected. Tsur-Lavie and Denekamp, (1982) present an argument against the Weakest Link Theory: "As a physical explanation for size effect, The Weakest Link Theory is based on the assumption that local rupture will extend into total failure. This is at variance with evidence indicating that multiple failure precedes total collapse." However, the authors mention that Weibull's formula has been widely used and generally a good fit is found with experimental data.

Weibull's formula is given by the following relationship:

$$m \log\left(\frac{\sigma_{c1}}{\sigma_{c2}}\right) = \log\left(\frac{V_2}{V_1}\right) \quad \text{Equation 3-1}$$

Where

m = material coefficient

$\sigma_{c1}$ ,  $\sigma_{c2}$  = Cubic strength of the respective volumes ( $V_1$ ) and ( $V_2$ ).

Brady and Brown (1999) also disagree with the Weakest Link Theory and state: "A popular approach is to interpret size effects in terms of the distribution of flaws within the material. Much of the data on which conclusions about size effects are based, were obtained using cubical specimens. Brown and Gonano (1975) have shown that in these cases, stress gradients and end effects can greatly influence the results obtained. The most satisfactory explanations of observed size effects in rock and other brittle materials are those in which surface energy is used as the fundamental material property."

Brady and Brown (1999) go on to explain that the surface energy concept originated from Griffith (1924), when he extended his tensile crack theory to compressive stresses, concluding that: "The use of Griffith's essentially microscopic theory to predict the macroscopic behaviour of rock material under a variety of boundary conditions, requires the introduction of a set of Griffith crack size, shape and orientation distribution functions which have not yet been defined."

The surface effect is described by Jackson and Lau (1990): “As the specimen diameter decreases, the larger surface area to volume ratio’s cause surface imperfections to have a greater impact resulting in undue stress concentrations and a lowering of the compressive strength.” They conclude that this type of effect will only be present if the surface imperfections are the dominant characteristics of the test specimen. Da Silva and Born (1993) suggest that hard, homogenous rocks may present an initially increasing than decreasing scale effect on the UCS, if these rocks contain discontinuities, which are rather spaced. This trend was observed (Baker-Duly, 1995) to occur in both heterogeneous Merensky reef (Figure 3-1), and on homogenous anorthosite rock. Baker-Duly (1995) postulated that the surface effects dominated sample strength for sample with diameters smaller than 50mm and so ignored the strengths of the 12 and 25 mm samples, and defined the relationship between scale and strength for Merensky by taking the strength values of samples with diameters larger than 50mm and smaller than 160mm (Figure 3-2).

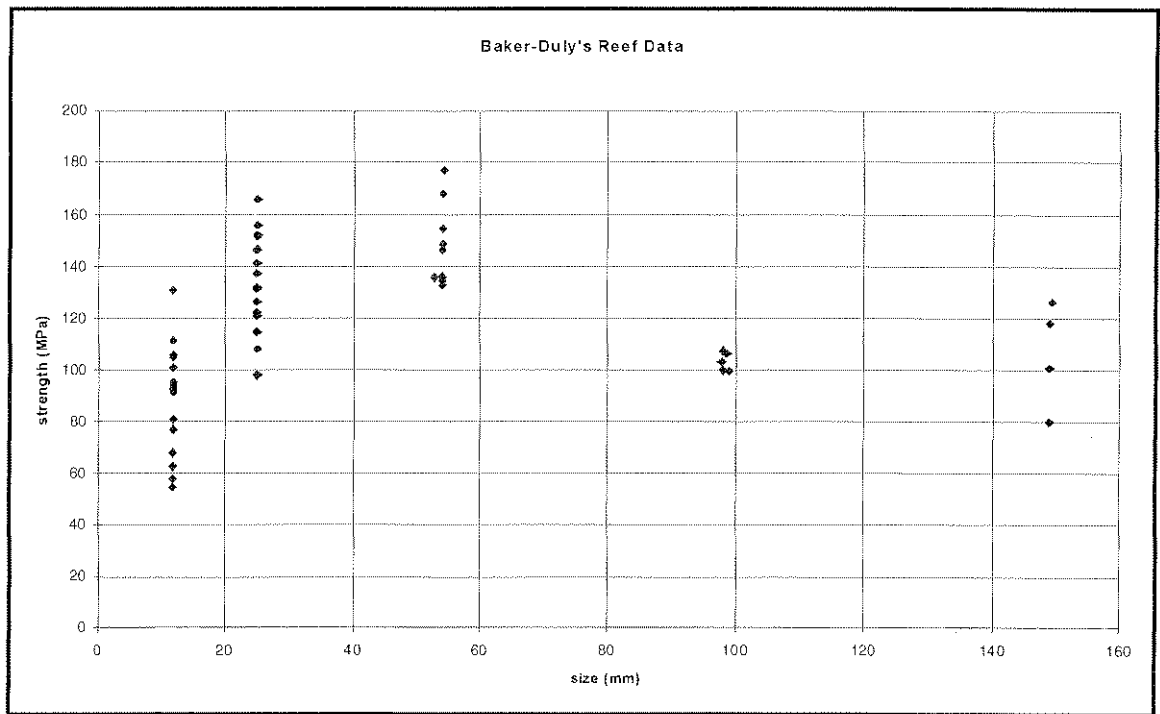


Figure 3-1: Surface-effects on Strength of Merensky Reef (Baker-Duly, 1995).

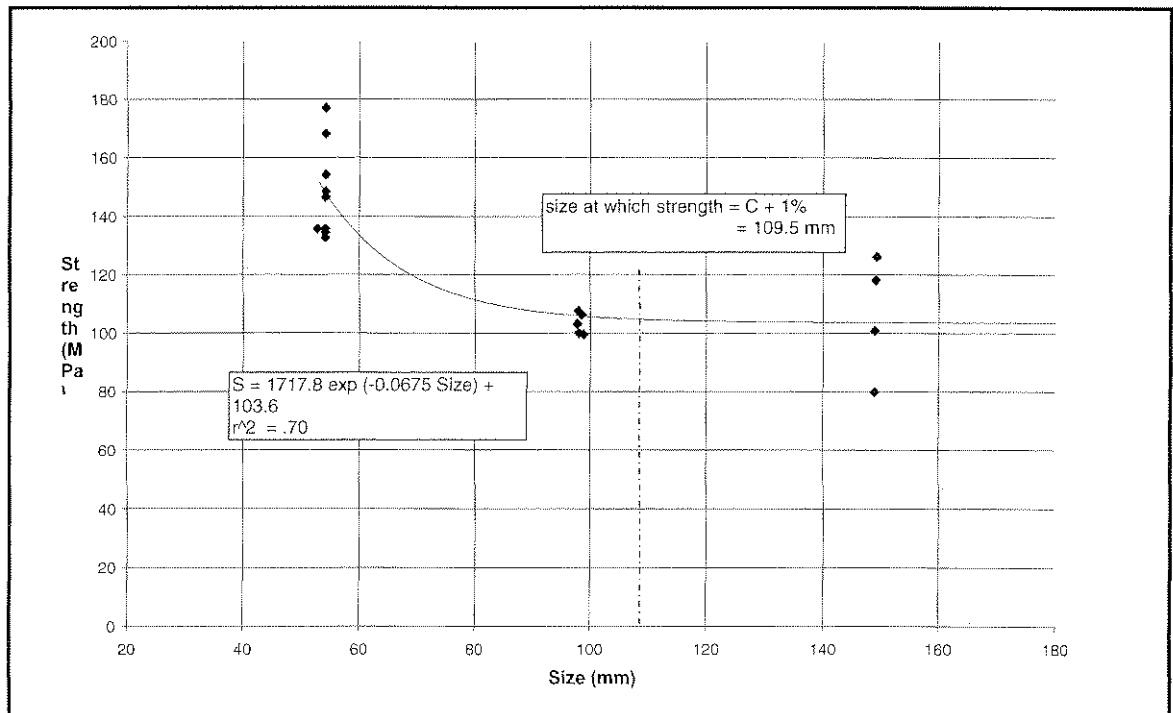


Figure 3-2: Scale effects observed for Merensky Reef Rocks, after York (1998)

Cunha (1990) states that scale effects on intact rock are essentially due to heterogeneity. Heterogeneity increases when:

- The number of different mineral components increase.
- There is significant variation of characteristics among the mineral components.
- There are great differences in the size of the components.
- Non-uniformity of the mineral distribution increases (That is, instead of a random distribution of all the mineral components in the volume, there are concentrations of certain components at different points).

The size effect is explained (Glücklich and Cohen,1968) by the amount of stored strain energy present, both in the sample and in the testing machine (under loading conditions). Glücklich and Cohen (1968) tested cylindrical gypsum plaster samples, having a length to diameter ratio (L/D) of 2, in series with a spring. They found that the strength indicated by these tests was 30 percent lower than usual. The authors mention that it is the amount of stored energy available within the system (i.e. machine and specimen) that determines whether the sample will fail prematurely or not. In the case of a hard system “little energy is stored and hence the energy-release rate does not exceed that of energy absorption.” However, in the case of a soft system, much energy is stored and the energy-release rate exceeds the absorption rate. Consequently much kinetic energy is formed and this results in a significant strength reduction.

However, Labuz and Biolzi (1991) concluded that once deformation localises within the sample, the stiffness of the machine is not the sole factor in determining a stable or unstable response. This conclusion follows experimental work undertaken on 26mm and 52mm notched Indiana limestone specimens ( $L/D = 2$ ) loaded under uniaxial compression. The authors found that stability is size dependent (Figure 3-3).

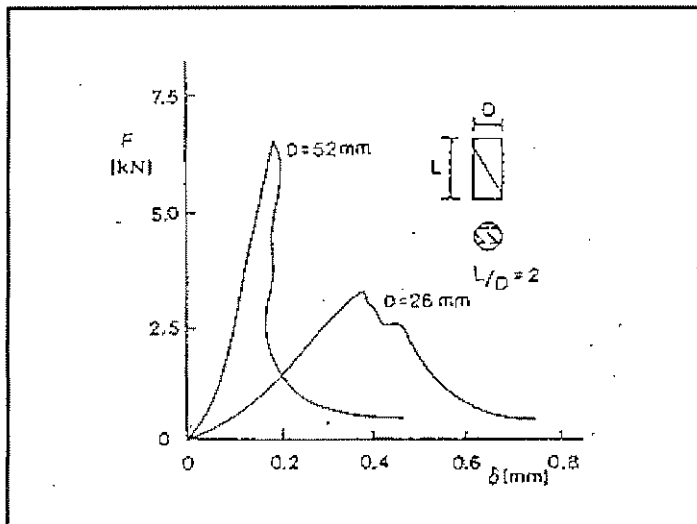


Figure 3-3: The size effect of two uniaxially loaded, notched-cores (after Labuz and Biolzi, 1991)

Thus a critical size exists such that a compression element composed of strain softening material may behave in an unstable manner. This is confirmed by Exadaktylos and Tsoutrelis (1993), who after performing experiments on Pendeli marble with varying crack densities, also found stability to be size dependent.

However, there is some controversy as to the existence of the scale effect. Brown (1971) [Quoted by Baker-Duly (1995)] indicated that the general comparisons between different specimen sizes are not valid because of the variable stress gradients resulting from specimen size and geometry, and testing conditions. He proposed that if scale effects were to be studied as an intrinsic property of the rock, as near to uniform loading as possible would need to be applied.

Brown, confirmed his argument by using results obtained from Hodgson and Cook (1970), who found no significant scale effect on specimens of quartzite and quartzitic shale (length to diameter  $(L/D) = 3$ ), under uniform loading.

Hudson *et al.* (1971) also found no scale effect on the UCS of Cherokee marble (under uniform loading conditions) for various  $L/D$  ratios. They mentioned that (under uniform loading) hard rock, relatively free of micro fracturing, is unlikely to show a strength size effect other than a possible one arising from the influence of strain energy stored within the failing rock.

Kramadibrata and Jones (1993) concluded that there is a significant strength scale effect for certain rocks under uniform loading ( $L/D = 2.5$ ), over a 30-150 mm size range. They found that rock specimens having a diameter of 150 mm or more approximated the in situ strength and noted that the size effect is more pronounced for hard brittle rocks than for soft rocks. This is in contradiction to Bieniawski (1972) who noted that the scale effects he observed were more pronounced in softer rock. He attributed this to softer

rocks such as coal, being having a high frequency of major cracks and other discontinuities, while these flaws are less prevalent in hard rocks.

Hoek and Brown (1980) on compilation of various hard rock results from previous investigators derived Equation 3-2.

$$\frac{\sigma_{cd}}{\sigma_{c50}} = \left( \frac{50}{d} \right)^{0.18} \quad \text{Equation 3-2:}$$

Where  $\sigma_{cd}$  is the UCS of a rock sample of diameter  $d$  (mm) and  $\sigma_{c50}$  is the UCS of a rock sample of 50mm diameter.

Hoek and Brown derived Equation 3-2: by normalising the stress with the UCS of the 50mm diameter specimen for each of the respective rock types. Data comparison was therefore made possible and this eliminated the differences due to specimen shape, loading rate, etc., since these factors are generally the same for a given set of data.

Other researchers agree however, that strength upon reaching a critical sample volume for a given rock type, become essentially independent of any further volume changes (Bieniawski, 1972; Pratt *et al.* 1972; Herget and Unrug, 1974; Kramadibrat and Jones, 1993). This is shown in Figure 3-4 and Figure 3-5, for coal, iron ore, norite and altered quartzitic diorite. Bieniawski and van Heerden (1975) stated that the size at which no further strength reduction occurs should be termed the critical size and the strength at this size the critical strength. 'This value is derived from a series





of laboratory or in situ tests on intact rock. The tests series either explicitly defines the critical size and strength, or the critical strength is obtained by extrapolation of the test data. An intact rock specimen, for hard rock implies no visible discontinuities. If the *in situ* pillar has no geological jointing, and minimal blast induced fracturing, the rock may be called intact. In this case, the critical strength may be taken as the *in situ* rock mass strength (York and Canbulat, 1998).'

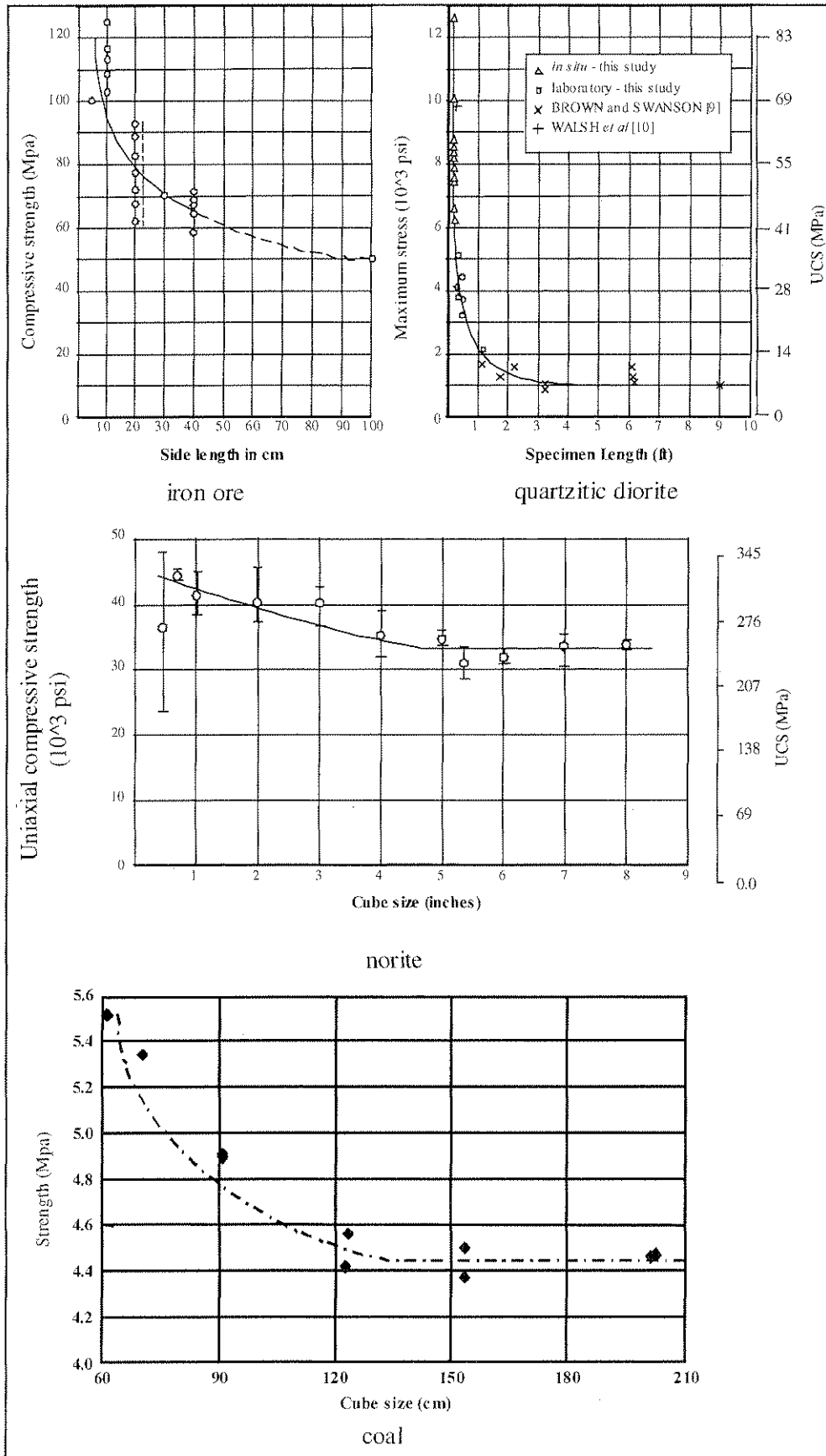


Figure 3-4: Scale effect as observed for different rock types (York and Canbulat, 1998).

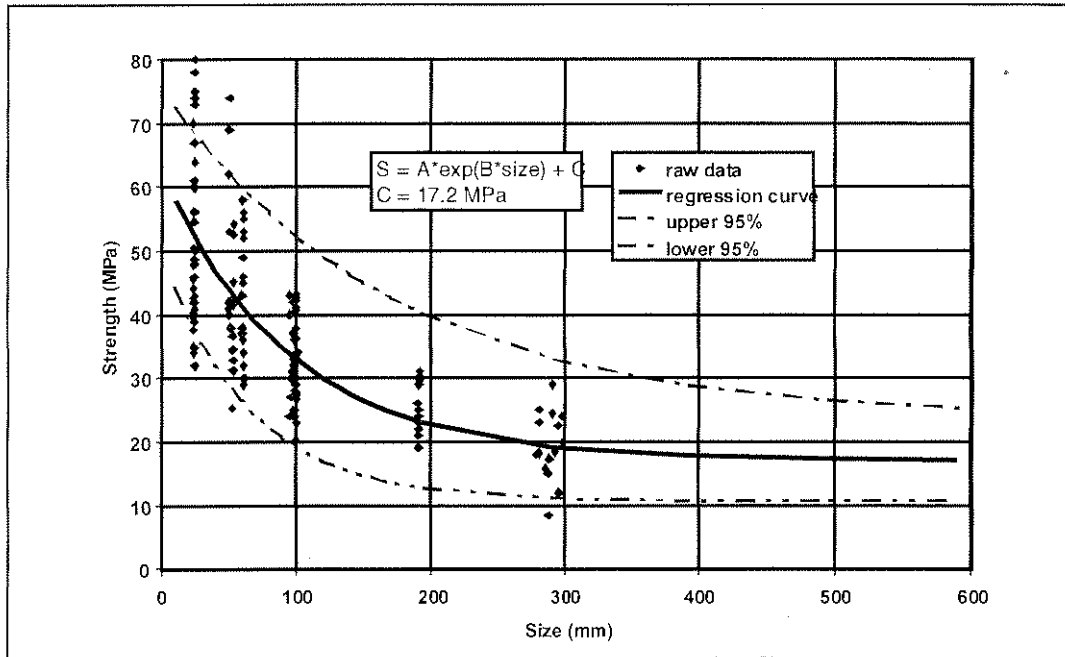


Figure 3-5: Scale effects on Coal (York and Canbulat, 1998).

### 3.2 The effect of w/h and contact friction angle on strength

The effect of w/h on strength has been found to be an important factor dictating rock strength of samples or pillars having w/h ratio's greater than 0.3 (Hawkes and Mellor, 1970). The cause for such a phenomena (i.e. strength increasing with increasing w/h ratio) has been suggested to arise mainly from the internal friction angle and the frictional conditions arising at the pillar contacts to the surrounding strata (Ozbay *et al*, 1994). For  $w/h \leq 6$  this strengthening effect has been found to be linear, and to vary in intensity for different rock types (Baker-Duly, 1995).

There is general agreement in literature (York *et al.*, 1999; Brady and Brown, 1999; Baker-Duly, 1995; Napier, 1990; Brown and

Gonano, 1974) that the underlying cause for the strengthening with increasing width to height ratio relationship is a result of friction between the loading platen and the specimen, providing lateral restraint and confinement to the specimen. Brown (1999) describes: “This confinement, for cylindrical specimens, penetrates into the specimen from either end in the form of conical lobes. With large width to height ratios these lobes overlap providing confinement to the full section height of the specimen thus increasing its strength (Figure 3-6).”

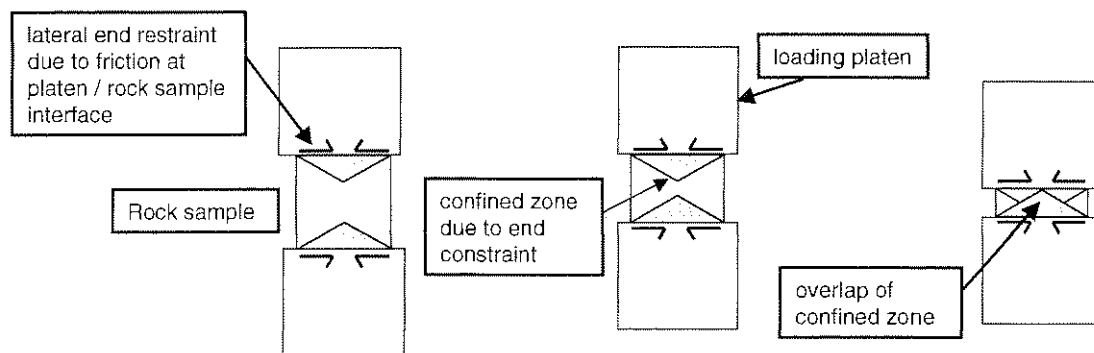


Figure 3-6: A conceptual diagram of the effect of frictional end restraint on the confinement of a sample, depending on its  $w/h$ .

The degree of strengthening with width to height ratio ( $w/h$ ) is rock type dependent (Baker-Duly, 1995).

### 3.3 Pillar strength equations

Pillar strength estimations are needed for mine pillar design purposes. These estimates can be obtained from laboratory work or by *in situ* back analysis of the pillar strengths in their mining environment. Much research has gone into the back analysis of

coal mine pillars, and this forms the bases of coal pillar design (Salamon *et al.*, 1997).

Pillars in underground mine workings are typically designed using an empirically derived strength formula. Typically, this is either a linear or power function.

The power formula is of the form:

$$S = kh^{\alpha}w^{\beta} \qquad \text{Equation 3-3}$$

Where  $k$ ,  $\alpha$  and  $\beta$  are numerically constants, determined by the back analysis of collapsed and intact pillars (Madden and Canbulat, 1997).

$S$  = the expected pillar strength

$h$  = the height of the pillar

$w$  = the width of the pillar.

The power formula (Equation 3-3) has found wide and consistent application in South Africa and Australia due to Salamon and Munro (1967). Their paper constitutes the most complete back analysis of *in situ* collapsed and intact pillars in underground coal mine workings. Several important principles regarding the linking of the Safety Factor concept with probability of failure were applied to the design of pillars.  $K$ ,  $\alpha$  and  $\beta$  were determined as 7,17 MPa, -0,66 and 0,46 respectively.

'Another approach has been to define a critical size, with an associated critical strength. This approach assumes that no further reduction of strength occurs with increasing size beyond a critical size (Bieniawski, 1975). Strength changes are then due to the geometry of the sample, as captured in the w/h ratio. The approach advocated by Bieniawski involves the definition of the critical strength for each coal seam dealt with and assumes a uniform strengthening effect due to geometry across all seams (York and Canbulat, 1998).' The linear formula proposed by Bieniawski and van Heerden (1975) is:

$$S = \sigma_c(c + m(w/h)) \quad \text{Equation 3-4}$$

where

$\sigma_c$  = the coal seams critical strength

S = the expected pillar strength

m = the slope of the linear function

c = the intercept of the linear function

w/h = the width to height ratio of the pillar.

The linear function as applied in coal pillar design was substantiated by Bieniawski and van Heerden (1975). Their function was based on *in situ* tests, with the use of a concrete platen at the top of the specimen. The base of the specimen was in the natural state.

Laboratory test results indicate that strength as a function of w/h ratio, for w/h ratios less than 4, are well explained by a linear fit (e.g. for coal, sandstone, and hard rocks, such as Merensky Reef, norite and anorthosite, York and Canbulat, 1998).

Above a certain value of w/h, the strength increases exponentially (the so-called “squat pillar” effect), with increasing w/h. To cater for this effect a squat pillar formula was derived by Salamon in 1982 (Salamon *et al.*, 1997).

$$S = k \frac{R_0^b}{V^a} \left\{ \frac{b}{\epsilon} \left[ \left( \frac{w/h}{R_0} \right)^c - 1 \right] + 1 \right\} \quad \text{Equation 3-5}$$

where S = the expected pillar strength

$R_0$  = the critical w/h at which the squat pillar effect starts. Commonly assumed to be 5, due to the fact that no pillar had collapsed with a w/h greater than 3.75 until 1988 (Madden and Canbulat, 1997)

$\epsilon$  = is the rate of strength increase

a = a constant = 0,0667

b = a constant = 0,5933

V = pillar volume.

Conventionally, the squat pillar effect is assumed to occur at  $w/h \geq 5$ . In this range of w/h, Equation 3-3 and Equation 3-5 are invalid, and the “squat pillar” formula (Equation 3-5) is often used (Wagner

and Madden, 1984). Pillars with  $w/h$  ratios greater than 10 have not been tested to destruction, it must be recognised that neither linear nor power formula have been validated at  $w/h$  ratios greater than about 8 (Salamon, 1997).

In shallow to intermediate depth tabular hard rock mines in South Africa, the laboratory strengths are downgraded based on a rock mass rating, or a strength reduction factor to derive an *in situ* reef strength (York and Canbulat, 1998).

Some researchers suggest that strength values obtained in the laboratory cannot be utilised in a meaningful way in pillar design (Salamon *et al.*, 1997; Mark and Baron, 1996). They support strength values obtained from back analysis of pillars in the mining environment.

Currently rock mechanic practitioners estimate pillar strengths based on the methods mentioned above. Pillar systems designed on this bases are then adjusted *ad hoc* to account for other factors, i.e. the footwall behaviour, panel spans, loading conditions, etc., which have not thus far been explicitly defined in an holistic pillar system design procedure (York and Canbulat, 1998).

Much research has gone into determining the factors, which effect the strength of pillars (Salamon and Munro, 1967; Obert, 1967; Ozbay, 1994; Madden, 1984). Some of these (York *et al.*, 1999) are:



- 1) the pillar dimensions, including stoping width (these lead to the w/h ratio)
- 2) strength of the pillar material
- 3) contact conditions between the pillar and the hanging- and footwall
- 4) horizontal weak layers or partings in the pillar
- 5) k-ratio (the ratio of virgin horizontal to vertical stresses)
- 6) the length : width ratio
- 7) different heights in the same pillar, due to one side being adjacent to a gully
- 8) jointing in the pillar
- 9) brittleness of pillar material
- 10) local loading system (relative stiffness of pillar and foundation)
- 11) creep and other time effects.

These factors should be used in a holistic pillar system design procedure (Figure 3-7).



strength of 103 MPa. This strength and the strengthening effect due to  $w/h$ , is dependent on the jointing and degree of fracturing the sample has and the friction angle defining the contact between the samples and the loading platens.

From the literature search it is evident that further test work will have to be carried out to further examine the critical strength of the Merensky Reef and the effects of  $w/h$  on its strength for  $w/h$  greater than 4. These values can then be used in a holistic pillar design methodology as illustrated in Figure 3-7.

## 4 Research methodology

Merensky Reef samples were obtained from rock cores drilled from Amandebult Mine in the BIC. The samples were then cut and prepared for laboratory tests. Standard uniaxial and triaxial rock tests were done to ensure that the rock samples were representative of the Merensky Reef. The scale and width to height tests were done on Miningteks 25MN testing machine.

### 4.1 Introduction

110 Intact cylindrical Merensky Reef samples at various sizes where prepared.

The samples with w/h of 1 where strain gauged with two bi-directional strain gauges placed on opposite sides, on the mid point of the samples. Displacement transducers where used to measure vertical strains on all the tests. The contact friction angle between the samples and the loading platens was determined and used in numeric modelling to determine its effect on sample strength.

Aluminium samples with the same diameters as the rocks to be tested were prepared, and strain gauged to establish the reproducibility of the testing procedure. It was discovered that the press used needed a spherical seat arrangement to compensate for its platens being slightly unparallel. A spherical seat arrangement was tested and the reproducibility of the test procedure confirmed.

## 4.2 Sample preparation

The cores originated from two drill sites on the mine. Samples were obtained from haulage drilling, with holes orientated perpendicular to the reef. A picture of the rotary pneumatic drill rig drilling at a site is show in

Figure 4-1.

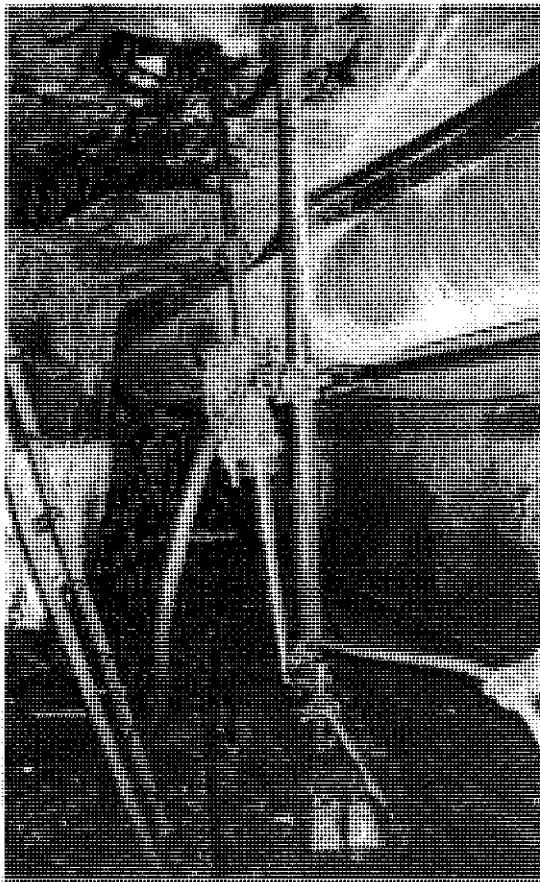


Figure 4-1: Coring of 54 mm Merensky Reef samples, using drill rig in a haulage.

Initially the Merensky samples cored were 250 mm in diameter. Other diameters were then derived from these cores. Subsequently the required core diameters were cored directly. The cores were then examined for major joints; core of the required length and diameter, free of major jointing was then cut and prepared (grinded) to the International Society of Rock Mechanics (ISRM) (1981)

surface finishing tolerance (specimen ends flat to 0.02 mm). A picture of a core cutting operation is shown in

Figure 4-2 and a sample grinding in

Figure 4-2.

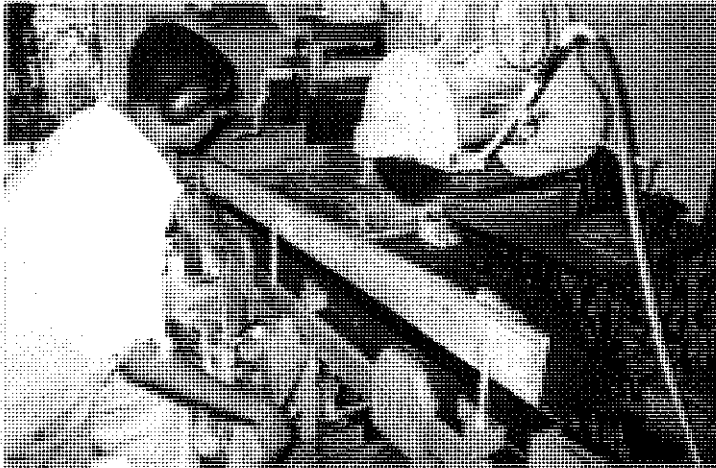


Figure 4-2: O. J. Mabena of CSIR Miningtek cutting core to the required test size.

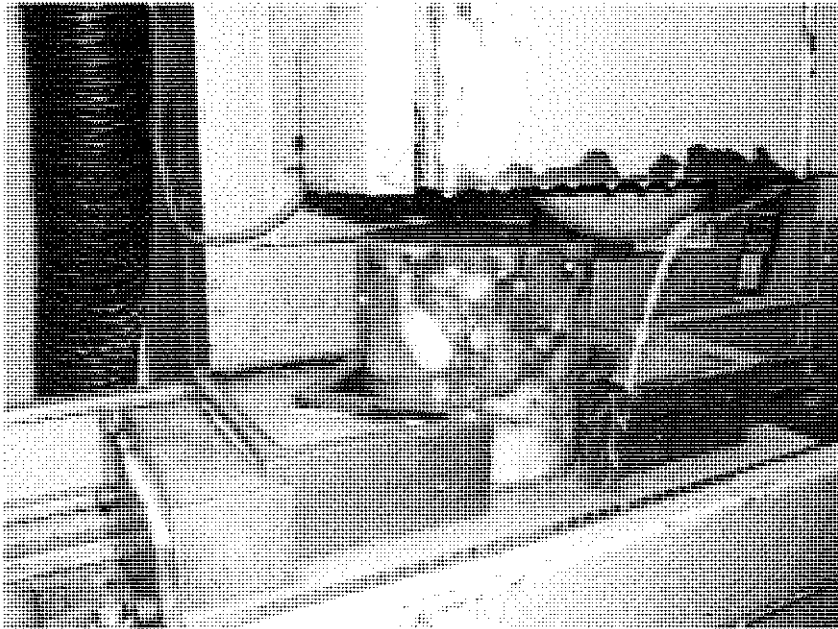


Figure 4-3: Sample grinding, CSIR Miningtek

The number of samples tested at different diameters and w/h are shown in Table 2. The samples with w/h = 1 were used to examine

the effect of scale, and all the samples were used to examine the effect of shape.

		Sample Diameter (mm)						Total No. of Samples
		50	76.5	101	125	151	250	
W/H	1	3	8	8	5	9	2	35
	2		4					4
	3	2	6	2		2	2	14
	4	2	6	2		2	2	14
	5	2	4					6
	6		6	2		2	2	12
	7		4					4
	8		4					4
	9		4					4
	10	2	6	1		2	2	13
								110

Table 2: Dimensions and the number of Merensky Reef samples tested.

### 4.3 Testing procedure

Due to the large sample diameters to be tested for the Merensky Reef, it was necessary to use a testing machine capable of very large compressive forces. The machine chosen for this was the 25 MN uniaxial, testing machine at CSIR Miningtek.

Platens for the test were made from EN30B steel, which was hardened to 48 Rockwell C. The platens were made approximately 5 mm larger in diameter than the samples and each had a  $w/h = 1$ .

This was to counter the effect of sample indentation into the platen and bending of the platen over the sample. Between each test the platens were reground to ensure that the friction angle between the sample and platen remained constant for each test. Soft-board 15 mm thick was placed between the machine platen and the top sample loading platen to act as a spherical seat for each test.

A displacement transducer was placed on opposite sides of each sample to record changes in sample length Figure 4-4. The strains recorded from the transducers were then to be correlated to the strains measured with the strain gauges, so that strains could be calculated for those samples not strain gauged.

The vertical deformation for each scale test was measured by means of strain gauges and transducers. The large grain size of the reef (up to 50 mm) resulted that the strain gauge readings were localized to the specific area to which they were attached. The strain gauge readings could therefore not be used. The transducer attachments under testing condition were also found to be faulty.



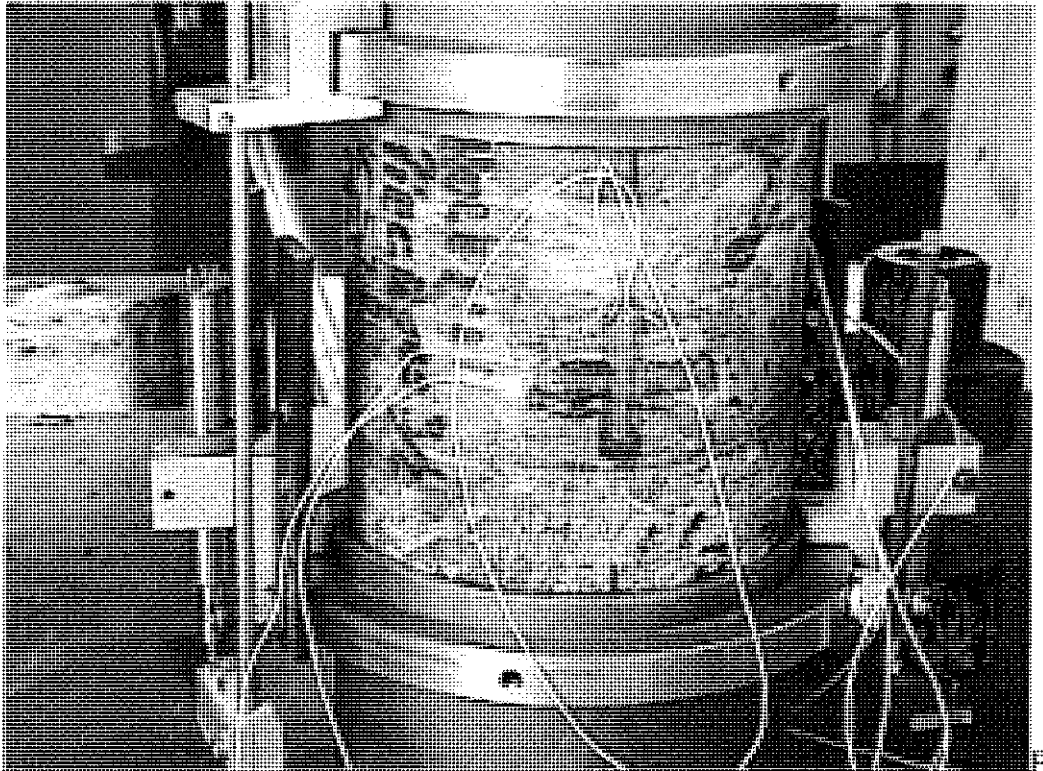


Figure 4-4: Test setup showing sample with strain gauges and transducers.

The machine was not servo controlled. A strain rate of 2.5 micro strain per second was strived for through the manual control of an electric motor loading the press, while monitoring a real time plot of the strain rate. The following readings were taken

- Peak compressive strength
- Loading rate
- Sample strain

## 5 Effect of scale

### 5.1 Introduction

As stated in section 3 the strength of rock samples of similar shape at different scales is not the same. Samples with diameters of 50, 54.5, 76.5, 101, 125, 151 and 250mm and with w/h ratios of 1 were prepared and tested (Table 2). The results of these tests are shown in Appendix C : Scale effect tests.

### 5.2 The effect of scale on strength

York and Canbulat (1998) concluded that the curve used to describe the effect of scale on strength should be of the form such that a term that decays with increasing size is added to a constant term, as follows:

$$S = [\text{strength decay with size}] + \text{constant term.}$$

If the form of the strength decay term is chosen such that it tends to zero with increasing size, the constant term becomes the critical strength. The strength decay term tending to zero is consistent with the notion of a critical size / critical rock mass strength. With this in mind, and with observation of the decay of the strength data with increasing size (Figure 3-4, Figure 3-5), the decay term was chosen to be exponential (York and Canbulat, 1998). The form of the function is therefore:

$$\Theta = A \cdot e^{(B \cdot \text{size})} + C \quad \text{Equation 5-1}$$

where  $\Theta$  = the strength of a sample of  $w/h = 1$

size = the diameter of the cylinder tested

A, B and C are regression parameters.

If various equations are fitted to the data by regression analysis, e.g. linear, power, exponential, quadratic, etc., the best fit is given by Equation 5-1 (Figure 5-1).

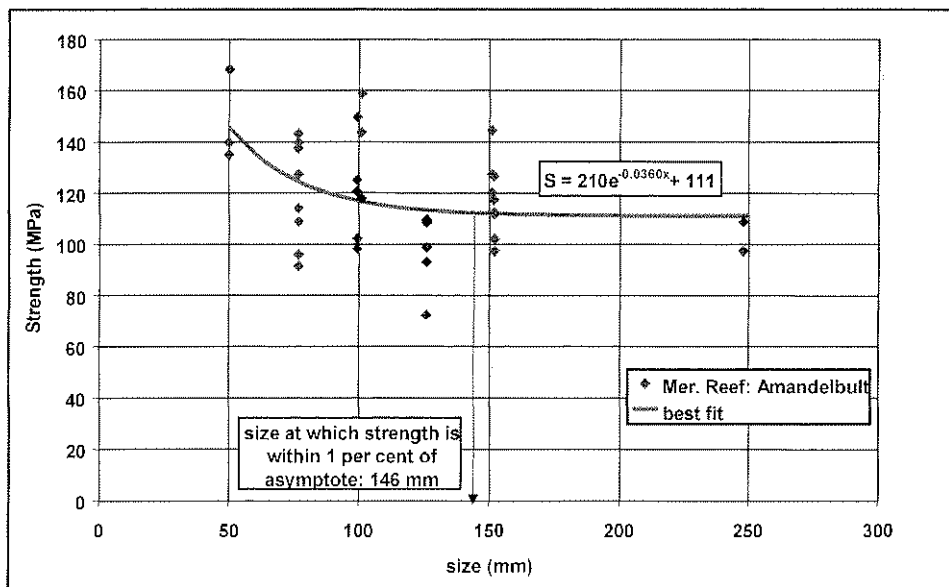


Figure 5-1: The strength – size relation for Merensky Reef samples from Amandelbult Platinum Mine.

The scatter observed in the results is expected because of the large grain size in the pyroxenite rock type, which on occasions is pegmatitic (G, York 1999).

Adding the tests results of Baker-Duly (1995) also on Merensky Reef samples but from Impala Platinum Mine, and fitting Equation

5-1 by regression analysis to the combined data, one gets the curve shown in Figure 5-2.

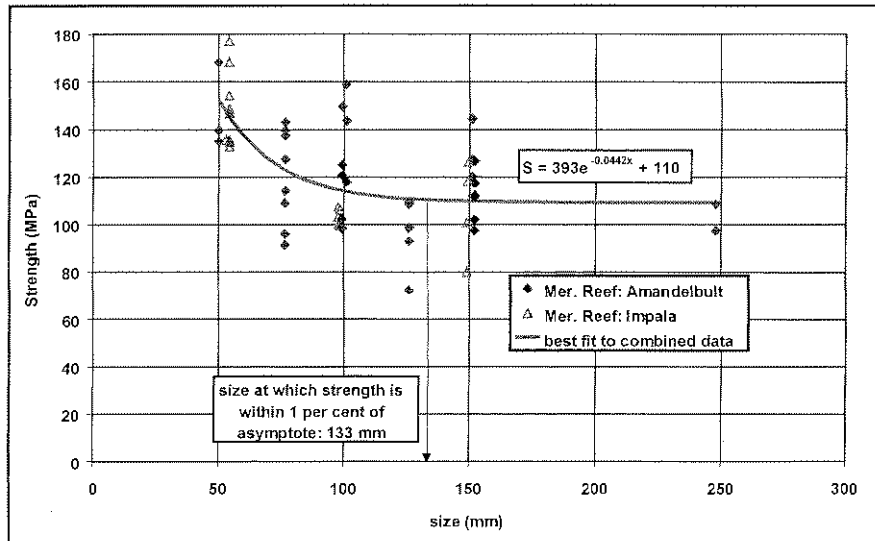


Figure 5-2: The strength – size relation for Merensky Reef from Amandelbult and Impala Platinum Mines.

The curves in Figure 5-1 and Figure 5-2 both specify a critical strength of about 110 MPa. The critical size though is smaller for the combined data at 133 mm. The critical size for this test series may therefore be safely taken from Figure 5-1 as 146 mm.

### 5.3 The effect of scale on sample failure pattern

The most typical observed failure pattern for these samples can be described as failures on planes. Failure initiates on planes of weakness, this then splits the sample, either in half if one plane dominates, or, if there are two planes, a wedge shaped cone forms

at the base of the sample. Figure 5-3 shows an intact sample before testing.

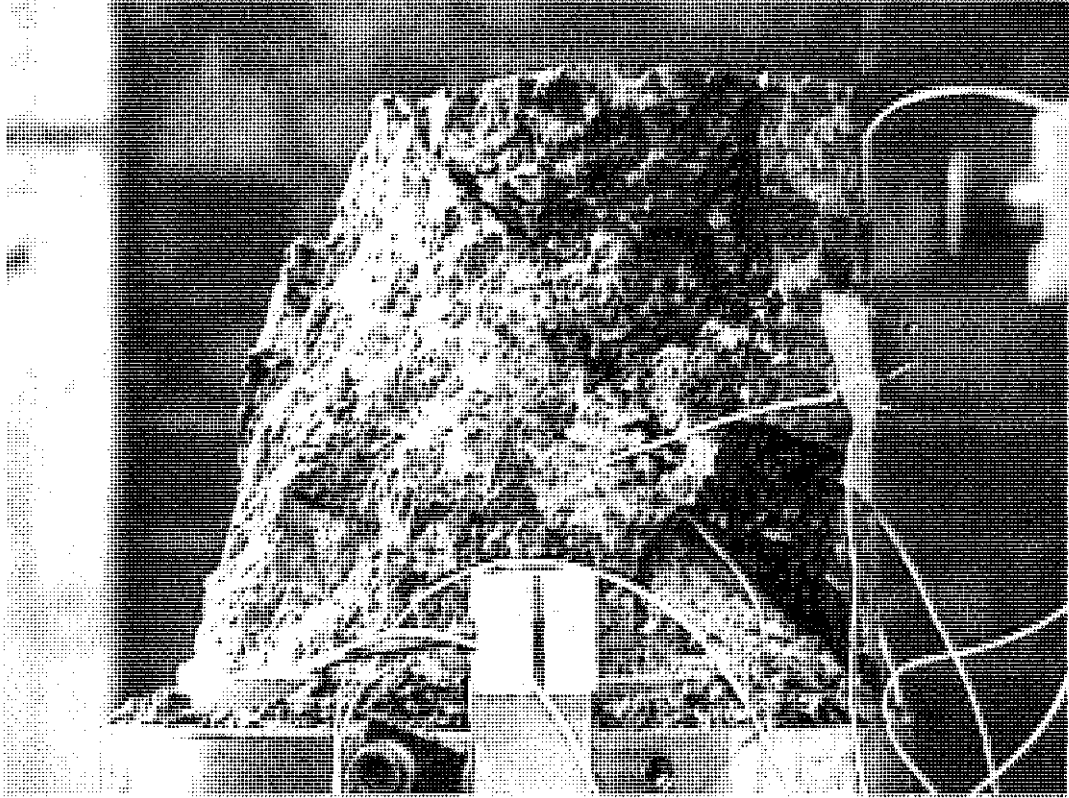


Figure 5-4 shows the same sample after testing, clearly showing the major failure plane.

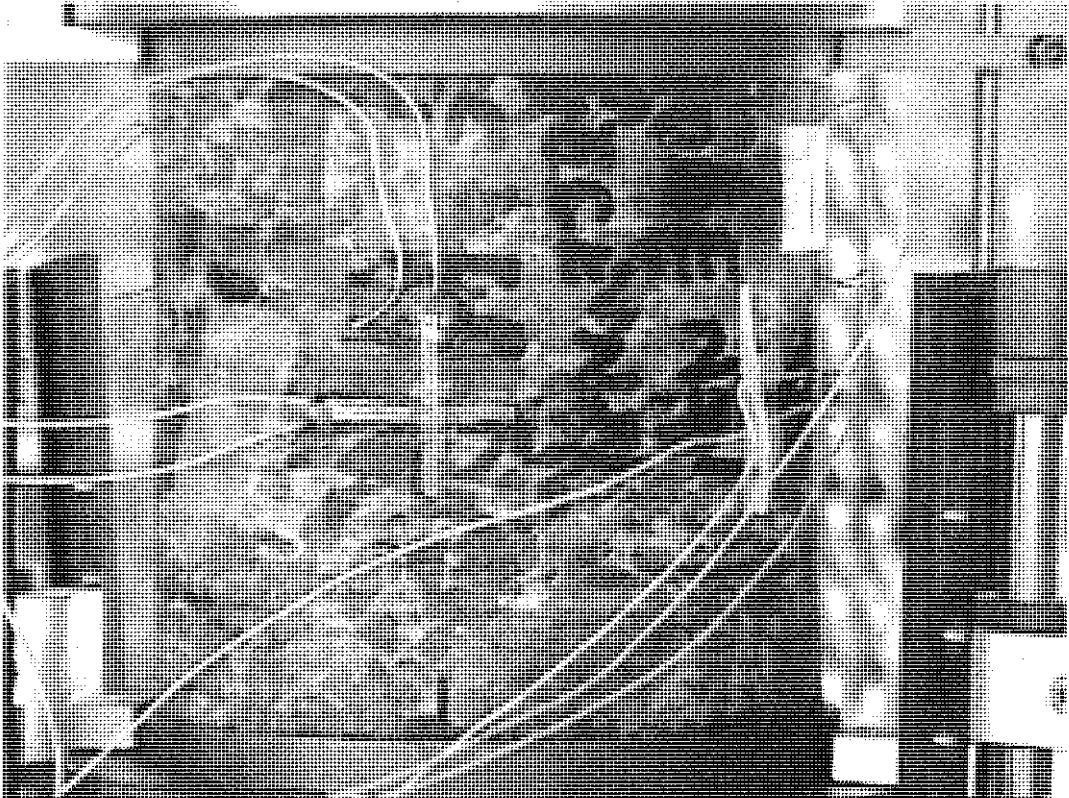


Figure 5-3: An intact sample (diameter = 126 mm, w/h = 1:1) before testing.

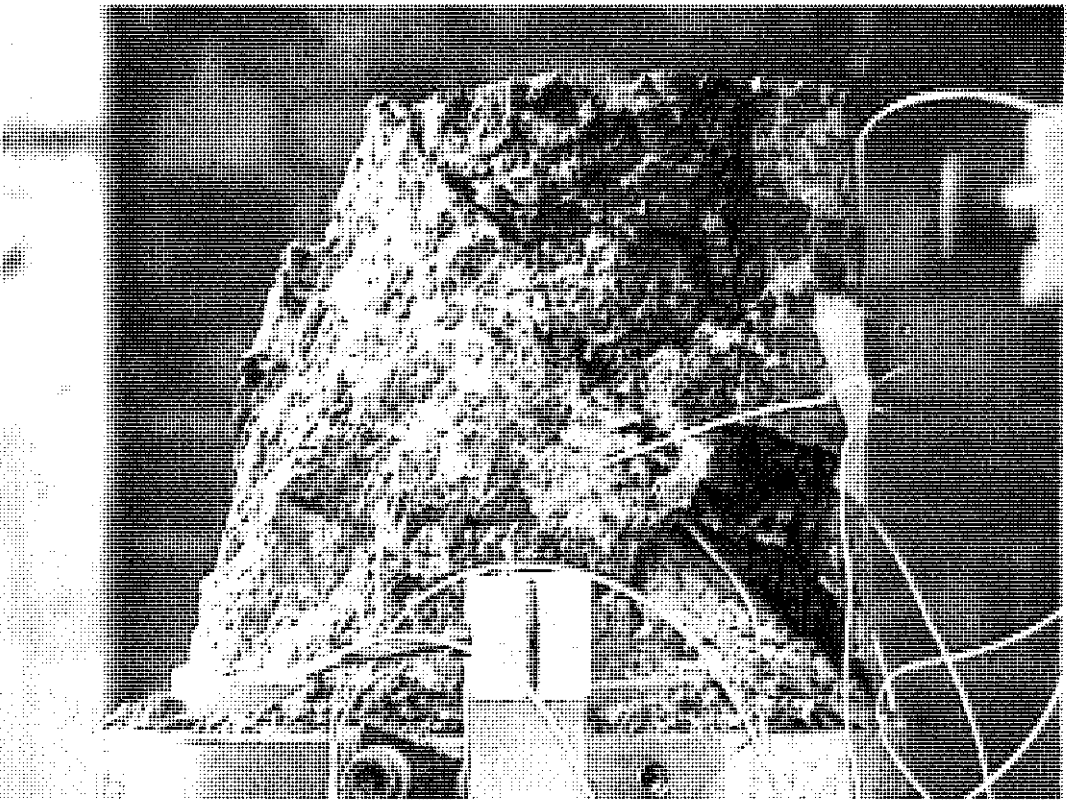


Figure 5-4: The sample in Figure 5-3 after testing showing failure along a plane.

Occasionally, a double cone or hourglass failure was observed (Figure 5-5), confirming the findings made in granite (Wawersik and Fairhurst, 1970). The cause of such failure arises from the friction at the sample/platen interface during loading, and has been well documented (Hawkes and Mellor, 1970; Vutukuri *et al.*, 1974; Wawersik and Fairhurst, 1970). Under increasing load, the friction inhibits the sample from expanding radially and thus the sample assumes a barrel shape. Simultaneously reinforced cones at either end of the sample develop. These are observed after sample failure.

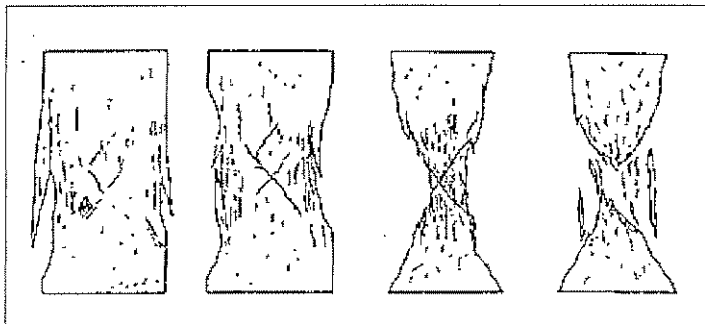


Figure 5-5: Schematic representation of failure development in Charcoal-grey-granite (after Wawersik and Fairhurst, 1970)

## 5.4 Conclusion

Under loading conditions described in 4.3 - Testing procedure, it is evident that Merensky Reef is scale dependent with a critical strength, having a 90 % confidence interval of between 100 and 120 MPa. It is important to emphasise that these results have been obtained with a specific set of boundary conditions. Differences in strength can be expected for different contact conditions.



The typical failure pattern of samples with a  $w/h = 1$ , is cone shaped. Hourglass failure patterns also occur.



## 6 Effects of w/h and the contact friction angle

### 6.1 Introduction

The dimensions and number of the samples tested to determine the effect of w/h on strength and deformation characteristics of Merensky Reef are shown in Table 2. The results of the tests are shown in Appendix D : *w/h effect tests*.

### 6.2 The effect of w/h on strength

Linear functions (Equation 3-4) were fitted by regression analysis to the data, for  $w/h \leq 6$ , as the data was clearly linear. This confirmed the linear effect of w/h on strength up to the w/h of 6. The results are shown in Table 3. The values of the regression parameters for the power formula (Equation 3-3) are shown in Table 4. The  $r^2$  values indicate the proportion of the total variation in strength that is accounted for by the variation of the independent variable/s in the fitted functions. The  $r^2$  values in Table 3 compare favourably with the  $r^2$  values in Table 4.

It is concluded that the linear function performs as well as the power formula.

Table 3: Linear functions (Equation 3-4) fits to  $w/h \leq 6$ .

Size (mm)	No. of samples	$R^2$	Linear function parameters	
			m	C
50	9	0.80	45.11	99.64
77	17	0.59	32.37	87.65
101	14	0.90	44.28	77.22
151	13	0.95	27.01	90.40
248	8	0.91	25.60	79.34

Table 4: Results of a power formula (Equation 3-3) fits to  $w/h \leq 6$ .

K	$\alpha$	$\beta$	$r^2$
78.4041	-0.4605	0.2775	0.80

In the above analysis, a separate linear function was fitted for each diameter, while the same power formula parameters were applied for all diameters. This demonstrates the ability of the power formula to handle volume. Conversely, it is demonstrated that the linear function is comparable to the power formula if the volume range is comparatively small. A similar result has been shown for coal laboratory and *in situ* data (York and Canbulat, 1998). Galvin *et al* (1996), in a statistical comparison between the power formula and the linear function on a set of Australian and South African coal

pillar collapse cases, showed that the difference between the two formulae is not statistically significant.

An example of the strength – w/h relation is shown in Figure 6-1, for samples of 250 mm diameter. The relation is clearly linear.

The fitted parameters of Equation 3-4 (Figure 6-1):

$m = 25,60$  and  $c = 79,34$ . The increase in strength for each unit increase in w/h is 25,60 MPa.

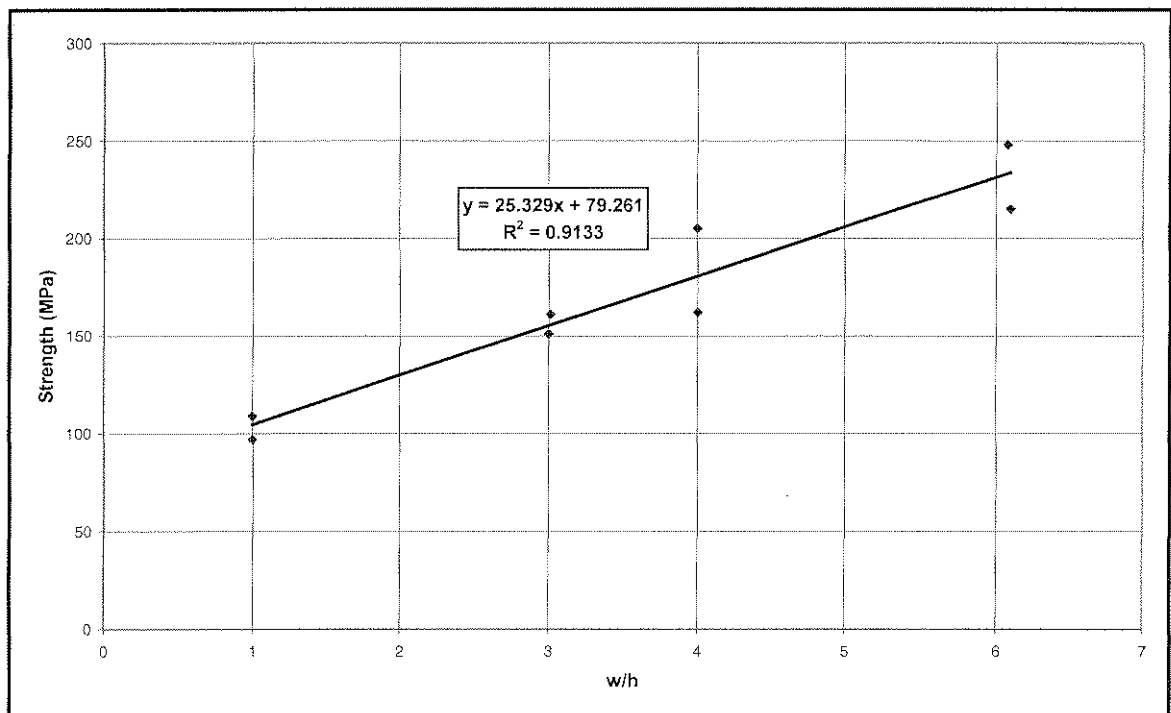


Figure 6-1: The strength – w/h relationship for Merensky Reef from Amandeubult Platinum Mine, for cylinders of diameter = 250 mm.

Initially only the test for w/h ratios of 1, 3, 6 and 10 were done for the all sample diameters shown in Table 2, except for the 125 mm diameters as these were only used in the scale effect tests (the

50mm diameters the w/h ratio of 6 was accidentally grinded down to far and so became a w/h ratio of 5). Due to the limited number of points on each curve from a w/h of 6 to 10, no curve could be fitted with reliability to define the relationship between w/h and strength for w/h values from 6 to 10. In each case there were only 4 points to do this, two at a w/h of 6 and two at a w/h of 10. It was therefore decided to do an additional series of tests. The new series consisted of 77 mm diameters for all w/h ratios from 1 to 10, with at least 4 tests at each w/h (Figure 6-2). 77 mm samples were chosen as these samples were large enough not be affected by surface energy effects and were easily obtainable from additional drilling.

The scatter of strength values for w/h above the value of 6 remained high. It was not possible to ascertain whether the strengthening effect could be described by a linear, power or other function.

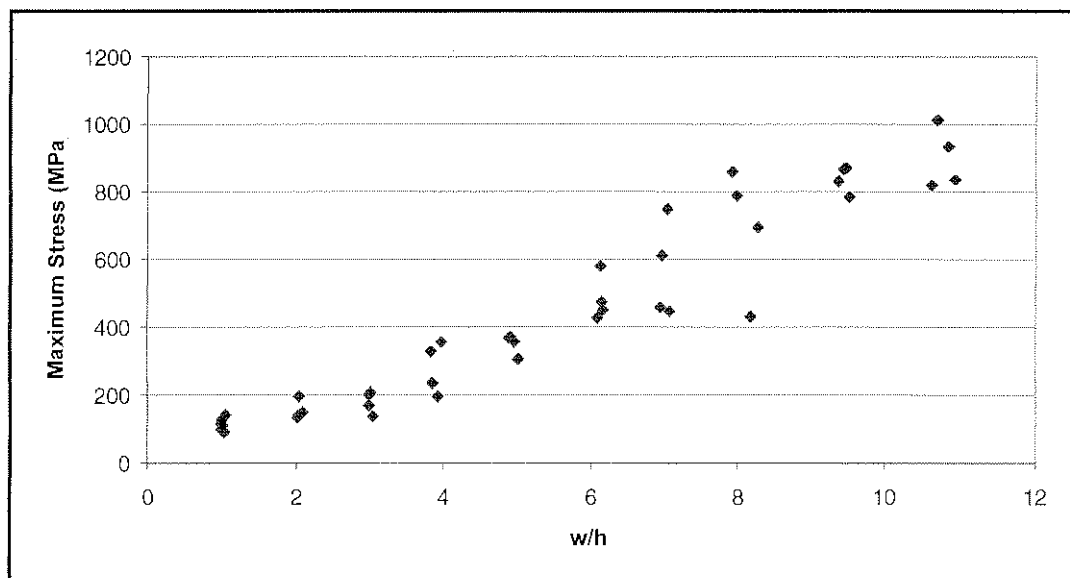


Figure 6-2: Additional w/h tests done on 77mm samples.

## 6.3 The effect of w/h on sample failure pattern

For samples having w/h ratios of 4 and above, plane, cone or hourglass type failure patterns are no longer observed. Tested samples display predominately concentric fracturing patterns arising from axial type fractures (Baker-Duly, 1995), as shown in Figure 6-3.

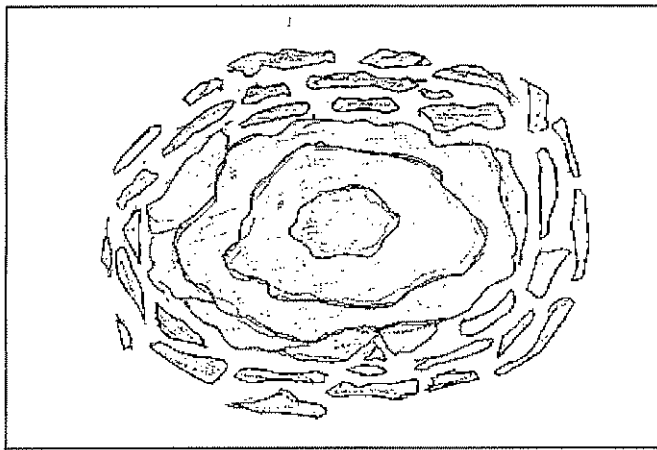


Figure 6-3: Concentric-fracturing arising from platen indentation effects (Baker-Duly, 1995).

The cause of such failure possibly results from cone interaction and reinforcement. In the case of samples having w/h ratios = 1/3 these cones are kept well apart to provide uniform a vertical stress distribution at the mid-height of the sample. However, at w/h ratios of four, cone interaction predominates and failure arises from axial type fractures. These commence from the outermost part of the sample – due to platen indentation effects – in the form of slabs. With increasing load further slabbing occurs until the sample finally collapses (Baker-Duly, 1995).

## 6.4 The effect of the frictional contacts on strength

The strengthening effect of  $w/h$  is generally ascribed to the increased confinement in the sample as  $w/h$  increases (Figure 6-4). However, the level of confinement must depend on the shear resistance at the loading platen / rock sample interface. This shear resistance, in turn, depends on the friction angle at the platen / sample contact. Therefore, a slippery contact should result in weaker samples, while a rougher contact should result in a greater  $w/h$  effect.

To test the effect of differing contact friction angles, the laboratory tests were numerically modelled using FLAC (York *et al.*, 1999). The FLAC model geometry is shown in Figure 6-5. The contact between the strain softening rock material and the elastic steel platen was varied from  $0^\circ$  (perfectly slippery) to  $30^\circ$ . The value of  $w/h$  was varied for each contact friction angle (Figure 6-6).

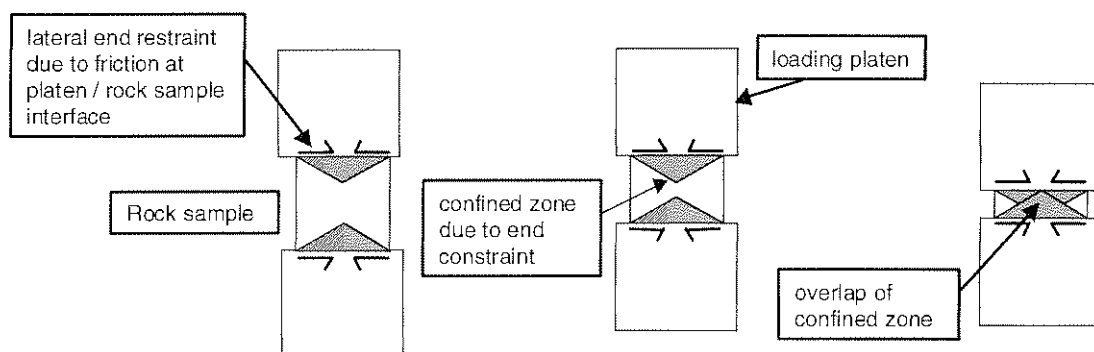


Figure 6-4: A conceptual diagram of the effect of frictional end restraint on the confinement of a sample, depending on its  $w/h$ .

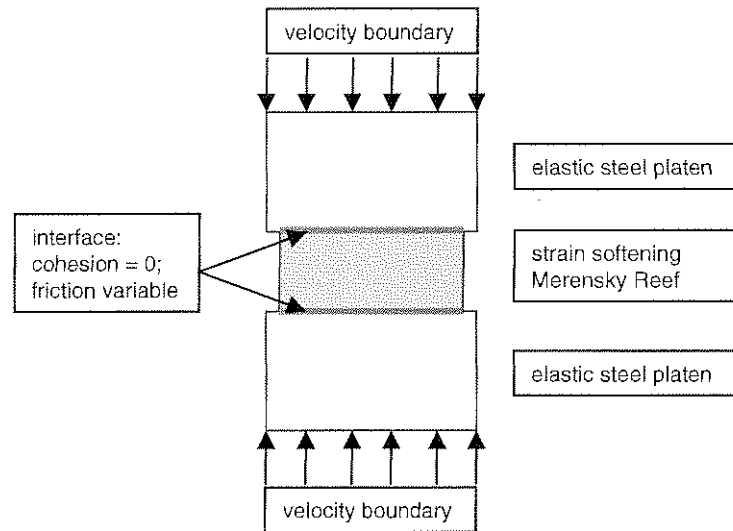


Figure 6-5: Geometry of FLAC model to test the effect of the contact friction angle on the strength of laboratory model pillars.

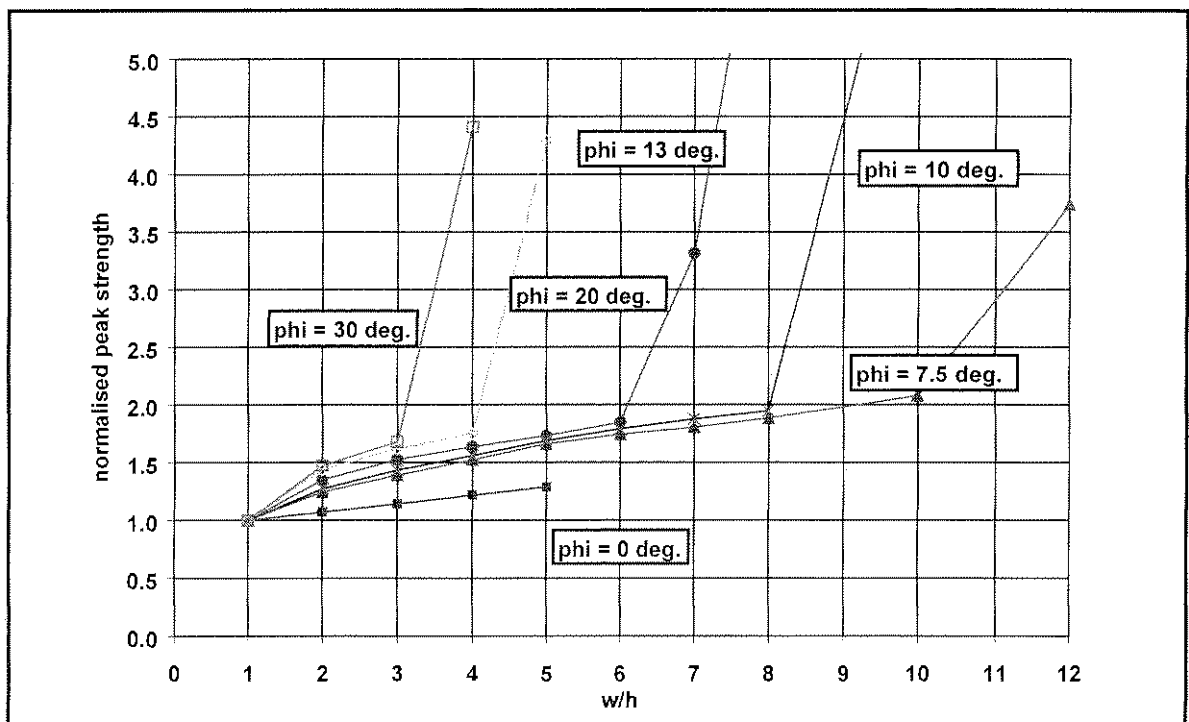


Figure 6-6: The effect of the contact friction angle on the w/h effect, on the basis of numerical modelling.

Three shear box tests were performed on the contact between Merensky Reef and steel platens. Both the Merensky Reef and the platens were surface finished to the normal standard required for

rock testing. The average value of the contact friction angle was  $13,7^\circ$ . A series of tests was performed on a friction angle testing bed, showing friction angles ranging between  $11^\circ$  and  $13^\circ$ . The laboratory test data points lie close to the curve predicted by the numerical modelling by York *et al.*, 1999. The agreement between the theoretically modelled curve and the plotted points based on laboratory data provides some confirmation of the notion that the w/h strengthening parameter is related to the contact friction angle (York, 1999).

To determine the friction angle between the reef and the chromitite band, which marks its foot and hangingwalls, 55mm in diameter core was drilled perpendicular through the reef into the hanging wall. Samples of intact specimens containing the contacts were prepared and tested in shear boxes. The results of three tests gave a friction angle of  $30.86^\circ$ . This friction angle is higher than the  $13,7^\circ$  determined for the laboratory samples tested. The effect of the difference between the laboratory and *insitu* friction angle must be considered when determining pillar strengths based on laboratory tests.

## 6.5 Conclusions

From the w/h tests the following conclusions can be made regarding Merensky Reef sample properties.

- There is a definite linear relationship between the w/h of a sample and the samples ultimate strength for  $w/h \leq 6$ .



- For samples having  $w/h$  greater than 6, the samples strength increases as its  $w/h$  increases. An acceptable curve could not be fitted to describe this trend.
- The contact friction angle between the sample and the loading platen influences the ultimate strength of the sample. A rougher contact results in a greater  $w/h$  strengthening effect.
- There is a marked difference in the *insitu* and laboratory contact friction angles for Merensky Reef.

## 7 Conclusions

The effects of scale and the  $w/h$  ratio on the strength for Merensky Reef have been further examined. The following are the major findings of this study.

- Under laboratory loading conditions Merensky Reef samples are scale dependent with a critical size of less than 150 mm and a critical strength, having a 90 % confidence interval of being between 100 and 120 MPa.
- The typical failure pattern of samples with  $w/h$  ratios less than 4 is cone shaped, but some hourglass failure patterns do occur.
- Samples having  $w/h$  ratios of 4 or greater, under laboratory loading conditions, fail concentrically towards their centres.
- The effect of the  $w/h$  ratio on strength has been confirmed to be linear until a  $w/h$  ratio of 6. For  $w/h$  greater than this strength continues to increase with increasing  $w/h$ .
- The contact friction angle between the sample and the loading platen influences the ultimate strength of the sample. A rougher contact results in a greater  $w/h$  strengthening effect.

These findings can be used in a pillar design methodology (Figure 3-7) to scientifically design pillar systems on the Merensky Reef horizon.

## 8 Acknowledgements

Acknowledgements go to:

- The Safety In Mines Research and Advisory Committee who funded the research project (GAP 334) from which this thesis was derived.
- Gary York and Dr. G.S. Esterhuizen for their patience and guidance.

## 9 References

- Baker-Duly, C.B., 1995. The effect of width to height ratio and size on the strength of hard rock test specimens under uniaxial compression. M.S.c Thesis, University of the Witwatersrand. 120.
- Bieniawski, Z.T., 1972. Propagation of brittle fracture in rock, Proc. 10<sup>th</sup> Symposium on Rock Mechanics, Texas, 409-427.
- Bieniawski, Z.T., 1968. The effect of specimen size on the strength of coal pillars. Int. J. Rock Mech. and Min Sci., V5, 325-335.
- Bieniawski, Z.T. and Van Heerden, W.L., 1975. The significance of in situ tests on large rock specimens. Int. J. Rock Mech. Min. Sci. & Geomech. Abstr. V12, 103-113
- Brady, B.H.G. and Brown, E.T., 1999. Rock mechanics for underground mining. Second Edition 87 – 137.
- Brown, E.T. and Gonano L.P., 1975. An analysis of size effect behaviour in brittle rock. Proc. 2<sup>nd</sup> Aust.-NZ Conf. Geomech., Instn. Engrs. Aust., Sydney, 139-143.
- The Chamber of Mines, 1999. <http://www.bullion.org.za/bulza/educatn/Platinum.htm>
- Cunha, A.P., 1990. Scale effects in Rock Mechanics. Int. Workshop on Scale Effects in Rock Masses, Leon.

- Da Silva, L.A. and Born, H., 1993. The definition of intact rock and its application to the determination of the smallest spacing between discontinuities in rock masses. Int. Workshop on the Scale Effects in Rock Masses, Lisbon, 211-216
- Exadaktylos, G.E. and Tsoutrelis, C.E., 1993. Scale effects on rock mass strength and stability. Int. Workshop on the Scale Effects in Rock Masses, Lisbon, 101-110
- Galvin, J.M., Hebblewhite, B.K. and Salamon, M.D.K., 1996. Australian coal pillar performance. Int. Soc. Rock Mech. News J., V4, No.1
- Glucklich, J. and Cohen, L.J., 1968. Strain energy and size effects in a brittle material. Material Research and Standards, V8 pp17-18
- Griffith, A.A., 1924. Theory of rupture. Proc. 1<sup>st</sup> Congr. Appl. Mech., Delft, 55-63.
- Hawkes, I. and Mellor, M., 1970. Uniaxial testing on rock mechanics laboratories. Eng. Geol. V4, 177–285.
- Herget, G., 1988. Stresses in rock. Rotterdam, Balkema.
- Herget, G. and Unrug, K., 1974. Insitu strength prediction of mine pillars based on laboratory tests. Int. Cong. On Rock Mechanics 3, Denver, V2A, 150-55.
- Hoek, E., and Brown, E.T., 1980. Underground excavations in rock. London, Imm.

- Hodgson, K. and Cook, N.G.W., 1970. The effect of size and stress gradient on the strength of rock. Proc. 2<sup>nd</sup> Int. Soc. Rock Mech. V2.
- Hudson, J.A., Brown, E.T. and Fairhurst, C., 1971. Shape of the complete stress-strain curve for rock. Proc 13<sup>th</sup> Symp. Rock Mech., Illinois, 773-795.
- ISRM, 1981. Suggested method for determining uniaxial compressive strength and deformability of rock materials. In: Rock Characterisation testing and monitoring ISRM Suggested Methods, ED. E.T. Brown, pergamon Press, London, 113-119
- Jackson, R. and Lau, J.S., 1990. The effect of specimen size on the laboratory mechanical properties of Lac du Bonnet grey granite. Theme 1. Int. Workshop on scale effects in rock masses, Leon.
- Kostak, B. and Bielenstein, H.U., 1971. Strength distribution in hard rock. Int. J. Rock Mechanics, V8, 501-21.
- Kramadibrata, S. and Jones, I.O., 1993. Size effect on strength and deformability of brittle intact rock. Int. Workshop on the Scale Effects in Rock Masses, Lisbon, 277-284
- Labuz, J.F. and Biolzi, L., 1991. Class 1 versus class 2 stability: A demonstration of size effect. Int. J. Rock Mech. Min. and Geomech. Abst. 28: 199-205

- Madden, B.J., 1984. The influence of width to height ratio on the strength and deformation of sandstone specimens. Research report, Chamber of Mines of South Africa.
- Madden B.J. and Canbulat I., 1997. Practical design considerations for pillar layouts in coal mines. 1<sup>st</sup> Southern African rock engineering symposium proceedings, 557-559.
- Mark, C. and Barton, T., 1996. The uniaxial compressive strength of coal : Should it be used to design pillars? 15<sup>th</sup> Int. Conf. On Ground control in Mining, Colorado.
- Obert, L. and Duvall, W., 1967. Rock Mechanics and Design of structures in rock. John Wiley & Sons, New York.
- Ozbay, M.U., Ryder J.A. and Jager A. J., 1995. The design of pillar systems as practised in shallow hardrock tabular mines in South Africa. J.S.Afr.Inst.Min Metall., V1.
- Ozbay, M.U., Ryder, J.A. and Jager, A.J., 1994. Miningtek report.
- Pratt, H.R., Black, A.D., Brown, W.S., and Brace, W.F., 1972. The effect of specimen size on the mechanical properties of unjointed diorite. Int. J. Rock Mech. Min. Sci., V9 513-529.
- Salamon, M.D.G., Galvin, J.M. and Hebblewhite, B.K., 1997. Pillar design – A review of South African and Australian Databases and development of an integrated pillar strength determination.

- Salamon, M.D.G. and Munro, A.H., 1967. A study of the strength of coal pillars. J.S.Afr. Inst. Min. Metall., V67.
- Stephenson, D.E. and Triantafilides, G.E., 1974. Influence of specimen size and geometry on the uniaxial compressive strength of rock. Bull. Assoc. of Eng. Geol. V11, No.1, 29-47
- Tsur-Lavie and Denekamp, S.A., 1982. Comparison of size effect of different types of strength tests. Rock Mechanics, V15, 234-254
- Vutukuri, V.S., Lama, R.D. and Saluja, S.S., 1974. handbook on the mechanical properties of rocks, V1, Trans. Tech. Publ.
- Wagner, H., 1974. Determination of the complete load deformation characteristics of coal pillars. Proc. 3<sup>rd</sup> Cong. Int. Soc. Rock Mech., Denver, CO, USA. 1076-1081
- Wagner, H. and Madden, B.J., 1984. Fifteen years Experience with the Design of coal pillars in shallow South African collieries. Design and Performance of Underground Excavations. ISRM, Cambridge.
- Watson, B.P., 1999. Determination of the influence of Rock mass parameters on the stability of panels between pillars. Part of technical note in SIMRAC project gap 334.
- Wawersik, W.R. and Fairhurst C., 1970. A study of brittle rock fracture in laboratory compression experiments. Int. J. Rock Mech. Min. Sci., V7, No 5.



- Weibull, W., 1939. A statistical theory of the strength of materials. Ing. Vetenskaps. Akad. Hanb. V151, 5-44.
- York, G., Canbulat, I., Kabeya, K., Le Bron K., Watson, B.P. and Williams, S.B., 1999. Develop guidelines for the design of pillar systems for shallow and intermediate depth, tabular, hard rock mines and provide a methodology for assessing hangingwall stability and support requirements for the panels between pillars. SIMRAC Final Project Report GAP334
- York, G. and Canbulat, I., 1998. The scale effect, critical rock mass strength and pillar system design. SAIMM. V1, 23-37.



## Appendices: Tests and results

## Appendix A: Standard tests

### Introduction

Standard tests were done on the Merensky Reef. These tests included uniaxial and triaxial tests as well as friction angle tests between the samples and the testing platens.

The angle of friction between the reef and the platens was determined to enable computer modelling of the tests. The cohesion and friction angle between the reef and a chromitite band, which forms the contact between the reef and the foot and hanging wall, was also determined so that this could be included in calculations before determining real pillar strengths.

### Uniaxial and triaxial tests

A summary of test dimensions and results is shown in Table 5. All samples were strain gauged.

The principle- stress diagram resulting from these tests is shown in Figure A-1. The tests reveal that the reef has the following Mohr-Coulomb parameters: angle of internal friction = 37.9 degrees, cohesion = 31.6 MPa and an UCS of 129.34 MPa. The Young's modulus the reef is about 95 GPa. These match findings of previous researchers (Watson, 1999). It is therefore concluded that the samples are representative of the Merensky Reef horizon.

Table 5: Uniaxial and triaxial strength tests Merensky Reef samples.



SPECIMEN PARTICULARS	SPECIMEN DIMENSIONS					SPECIMEN TESTS RESULTS					
	Dia (mm)	Height (mm)	Height to Dia Ratio	Mass (g)	Density (kg/m <sup>3</sup> )	Minor Principal Stress (MPa)	Strength (UCS/TCS) (MPa)	Tangent @ Poisson's Ratio	50% strength Deformation Modulus (GPa)	Modulus Ratio	Type of Failure
UCP-01	25.4	76.2	3.0	124.82	3230	0	130.9	n/a	103.5	791	XA
UCP-02	25.3	76.2	3.0	125.05	3260	0	119.6	n/a	101.1	845	XA
UCP-03	25.4	76.2	3.0	121.83	3160	0	119.5	n/a	87.0	728	XA
TCS-04	25.4	76.2	3.0	125.47	3250	10	170.4	0.34	83.9	492	XA
TCS-05	25.4	76.2	3.0	125.85	3260	20	193.7	0.25	86.5	447	XA
TCS-06	25.4	76.2	3.0	125.98	3260	40	302.1	0.26	134.2	444	XA
TCS-07	25.4	76.2	3.0	122.39	3170	10	186.9	0.26	85.7	459	XA
TCS-08	25.4	76.2	3.0	123.23	3190	20	220.5	0.35	83.9	380	XA?
TCS-09	25.4	76.2	3.0	120.71	3130	40	286.2	0.26	101.3	354	4B?
TCS-10	25.4	76.2	3.0	123.37	3200	10	190.9	n/a	87.7	459	XA
TCS-11	25.4	76.2	3.0	120.13	3110	20	209.9	0.32	88.6	422	XA
TCS-12	25.4	76.2	3.0	118.10	3060	40	302.1	0.34	89.7	297	XA

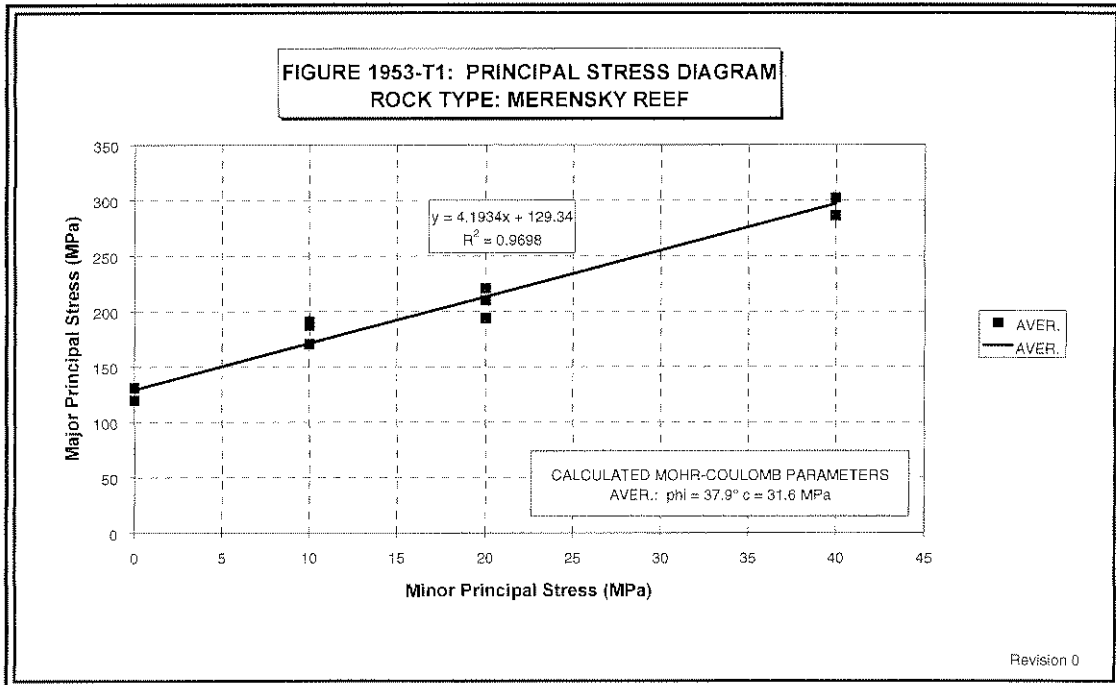


Figure A-1: Principal stress diagram for Merensky Reef.

## Friction angle tests

Baker-Duly (1995), reported the large influence on strength of contact friction angle between specimen and platen. He performed scale effect tests on anorthosite, pyroxenite and Merensky Reef, at normal platen rock contact friction angles (coefficients of frictions of 0.56, 0.62 and 0.64 were determined for anorthosite, pyroxenite and reef respectively). Tests were also performed at near to zero contact friction angles (coefficient of friction of 0.05). Average strength reduction of 49.2%, 57.9% and 57.2% were observed for the rock types respectively.

The friction angle between the samples and the loading platen was determined by shear box tests and tilt table tests. Three of the tests gave a friction angle average if  $13.7^\circ$ . One test was not included in this its value was considered too low ( $7.5^\circ$ ). The results are shown in

Appendix B : *Friction angle tests.*

Tests done between the rock specimens and the platens on a standard friction angle table indicate a friction angle of between 11 and 13 degrees. The platen was placed on the table, and the specimen on top of the platen. The table was then inclined by means of a threaded screw. The specimen was gently nudged at intervals. The angle at which the specimen started sliding freely along the platen was then recorded.

To determine the friction angle between the reef and the chromitite band, which marks its foot and hangingwalls, core was drilled perpendicular through the reef into the hanging wall. Samples of intact specimens containing the contacts were prepared and tested in shear boxes.

The results of these three tests gave a friction angle of  $30.86^\circ$ ; this value can now be used for pillar design purposes on the mine.



## Appendix B : Friction angle tests

Test name	Rock type/Interface	Shear properties	Cohesion (Mpa)	Fric.Angle	Notes
1995-sh-1	Pyroxenite/Chromite	Intact	362	67	Dry tested
1995-sh-01	Pyroxenite/Chromite	Residual	0	25.6	Intact determined in the same direction as residual values. Dry
1995-sh-02	Pyroxenite/Chromite	Residual	0	32.8	Intact determined in the same direction as residual values. Dry
1995-sh-03	Pyroxenite/Chromite	Residual	0	33.9	Intact determined in the same direction as residual values. Dry
1995-shs-03	Mremsky/Steel	Residual	0	15.6	Dry tested
1995-shs-05	Mremsky/Steel	Residual	0	14.1	Dry tested
1995-shs-04	Mremsky/Steel	Residual	0	11.4	Dry tested
1907-shs-51	Mremsky/Steel	Residual	0	7.5	
1907-shs-51	Anorthosite/Steel	Residual	0	7.6	

## Appendix C : Scale effect tests

Table 6: Scale effect tests on Merensky Reef.

Sample No.	Height (mm)	Width (mm)	w/h	MaxStress (MPa)	Strain Gauge Modulus (GPa)	Load Rate (MPa/s)
2	50.00	50.00	1.00	135.00	101.905	1.00
3	50.00	50.00	1.00	139.66		
1	50.03	50.00	1.00	168.27		
12	76.50	76.50	1.00	139.66	114.707	0.4763
13	76.50	76.50	1.00	137.43	73.29	0.2346
22	101.00	101.00	1.00	143.57	115.17	0.2771
23	101.00	101.00	1.00	117.88	102.58	0.2021
24	101.00	101.00	1.00	158.88		
32	151.00	151.00	1.00	144.47	104.52	0.1581
33	151.00	151.00	1.00	127.37	85.02	0.1534
34	151.00	151.00	1.00	120.11	100.75	0.2496
44	250.00	248.00	0.99	108.65	77.73	0.1209
43	252.00	248.00	0.98	97.38	110.58	0.1298
53	55.41	54.60	1.01	129.05	117.49	0.2212
54	55.63	54.60	1.02	111.08	98.62	0.10963
55	55.90	54.60	1.02	131.23		
56	56.10	54.60	1.03	122.96	99.28	0.1502
57	56.32	54.60	1.03	113.41	106.3732	0.1808
58	56.36	54.60	1.03	136.31	100.93	0.4154
59	77.50	76.50	0.99	114.18		
60	77.35	76.50	0.99	96.09	104.0068	0.353
61	77.25	76.50	0.99	127.37	114.04	0.2232
62	76.38	76.50	1.00	109.01	79.20	0.1506
63	74.78	76.50	1.02	91.44	97.09	0.1927
64	73.65	76.50	1.04	143.11	98.65	0.3775
101	100.37	99.30	0.99	102.23	80.06	0.1365
102	100.30	99.30	0.99	98.32	80.500	0.1453
103	100.11	99.30	0.99	125.14	121.21	0.1693
104	100.00	99.30	0.99	120.67	81.19374	0.1504
105	99.65	99.30	1.00	149.72	100.39	0.1835
106	125.23	126.00	1.01	72.33	95.44	0.1472
107	124.72	126.00	1.01	98.68		0.1148
108	124.00	126.00	1.02	109.53	62.403	0.1988
109	123.60	126.00	1.02	92.99	89.69	0.1718
110	122.43	126.00	1.03	108.49	71.47	0.1558
111	152.20	152.00	1.00	111.59	92.42	0.1751
112	152.00	152.00	1.00	102.09	73.94	0.2236
113	151.82	152.00	1.00	112.30	102.86	0.2814
114	151.45	152.00	1.00	126.62	123.38	0.1727
115	151.00	152.00	1.01	97.33	96.50	0.2111
116	151.00	152.00	1.01	117.38	86.28	0.19365



## Appendix D : w/h effect tests

Table 7: Results of w/h tests for series 1.

Series 1				
Test No	Width	Height	W:H	Max Stress
1	50	50.03	1.00	168.27
2	50	50.00	1.00	135.00
3	50	50.00	1.00	139.66
4	50	16.97	2.95	224.58
5	50	16.00	3.13	175.42
6	50	12.93	3.87	318.07
7	50	12.88	3.88	321.78
8	50	10.93	4.58	310.08
9	50	10.02	4.99	294.30
10	50	4.93	10.15	898.31
11	50	4.92	10.17	994.40
12	76.5	76.50	1.00	139.66
13	76.5	76.50	1.00	137.43
14	76.5	26.00	2.94	207.82
15	76.5	25.48	3.00	138.55
16	76.5	18.41	4.16	122.90
17	76.5	18.00	4.25	127.37
18	76.5	12.60	6.07	268.15
19	76.5	12.50	6.12	328.82
20	76.5	8.00	9.56	631.92
21	76.5	7.90	9.68	747.77
22	101	101.00	1.00	143.57
23	101	101.00	1.00	117.88
24	101	101.00	1.00	158.88
25	101	33.50	3.01	205.58
26	101	33.00	3.06	194.41
27	101	24.97	4.05	229.05
28	101	24.95	4.05	200.00
29	101	16.96	5.96	359.14
30	101	16.92	5.97	384.42
31	101	9.94	10.16	815.90
32	101	9.50	10.63	834.00
33	151	151.00	1.00	144.47
34	151	151.00	1.00	127.37
35	151	151.00	1.00	120.11
36	151	50.99	2.96	172.20
37	151	50.80	2.97	165.35
38	151	37.97	3.98	142.18
39	151	37.90	3.98	154.82
40	151	25.02	6.04	259.33
41	151	25.00	6.04	249.08
42	151	15.00	10.07	740.33
43	151	15.00	10.07	761.25



44	250	250.00	1.00	97.00
45	250	250.00	1.00	109.00
46	250	83.33	3.00	151.00
47	250	83.00	3.01	161.00
48	250	62.50	4.00	205.00
49	250	62.50	4.00	162.00
50	250	41.15	6.08	248.00
51	250	41.00	6.10	215.00
52	250	24.99	10.00	>400
53	250	25	10.00	>400



Table 8: Results of w/h tests for series 2.

Series 2				
Test No	Width	Height	W/H	Max Stress
60	76.50	77.50	0.99	114.18
61	76.50	77.35	0.99	96.09
62	76.50	77.25	0.99	127.37
63	76.50	76.38	1.00	109.01
64	76.50	74.78	1.02	91.44
65	76.50	73.65	1.04	143.11
66	76.50	37.83	2.02	132.26
67	76.50	37.55	2.04	140.01
68	76.50	37.50	2.04	197.35
69	76.50	36.60	2.09	148.79
70	76.50	25.55	2.99	170.49
71	76.50	25.53	3.00	198.39
72	76.50	25.35	3.02	208.72
73	76.50	25.08	3.05	138.46
74	76.50	19.88	3.85	327.55
75	76.50	19.80	3.86	236.10
76	76.50	19.43	3.94	197.87
77	76.50	19.20	3.98	356.99
78	76.50	15.60	4.90	368.88
79	76.50	15.55	4.92	371.98
80	76.50	15.35	4.98	356.48
81	76.50	15.20	5.03	305.85
82	76.50	12.55	6.10	425.71
83	76.50	12.48	6.13	581.47
84	76.50	12.45	6.14	476.28
85	76.50	12.40	6.17	452.41
86	76.50	11.00	6.95	458.06
87	76.50	10.98	6.97	612.63
88	76.50	10.88	7.03	747.53
89	76.50	10.83	7.07	447.06
90	76.50	9.65	7.93	859.39
91	76.50	9.60	7.97	788.73
92	76.50	9.35	8.18	433.24
93	76.50	9.25	8.27	693.17
94	76.50	8.18	9.36	831.78
95	76.50	8.10	9.44	864.89
96	76.50	8.08	9.47	871.71
97	76.50	8.05	9.50	785.03
98	76.50	7.20	10.63	820.09
99	76.50	7.15	10.70	1012.36
100	76.50	7.05	10.85	932.10
101	76.50	7.00	10.93	835.67